

ENVIRONMENTAL  
PROTECTION AGENCY

DEC 20 2006

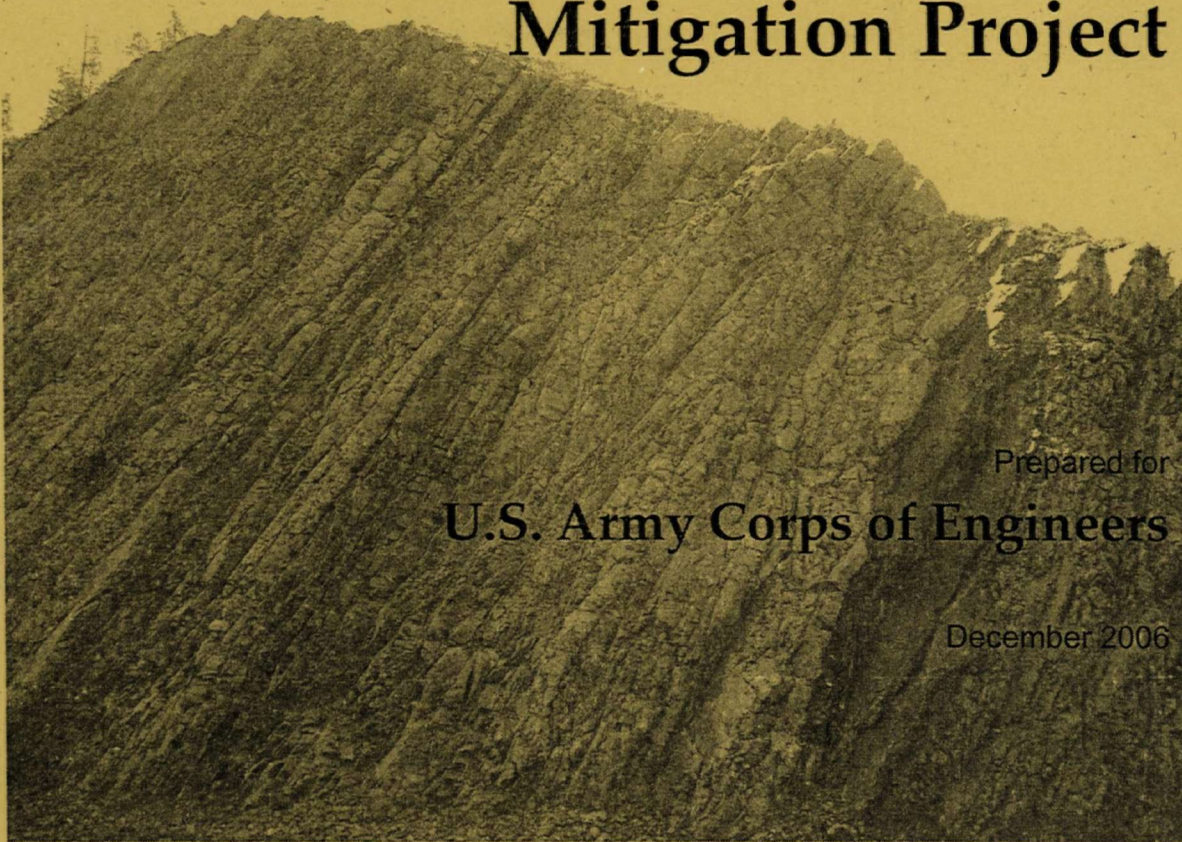
MONTANA OFFICE

1569930 - R8 SDMS

---

*Geotechnical Report*

# Geotechnical Report for the Milltown Reservoir Bridge Mitigation Project



Prepared for  
**U.S. Army Corps of Engineers**

December 2006

Prepared by

**CH2MHILL**

322 East Front Street, Suite 200

Boise, Idaho



# CH2MHILL TRANSMITTAL

ENVIRONMENTAL  
PROTECTION AGENCY  
DEC 20 2006  
MONTANA OFFICE

**To:** USACE, Seattle District  
1600 North Avenue West, Suite 105  
Missoula, MT 59807

**From:** Dennis Smith  
322 East Front Street, Suite 200  
Boise, ID 83702

**Attn:** Lynn Daniels

**Date:** December 19, 2006

**Re:** Geotechnical Report

**We Are Sending You:**

Method of shipment: FedEx

☒ Attached

Under separate cover via

Shop Drawings

☒ Documents

Tracings

Prints

Specifications

Catalogs

Copy of letter

Other:

| Quantity | Description  |
|----------|--|
| 1        | Geotechnical Report for the Milltown Reservoir Bridge Mitigation Report, December 2006 |

If the material received is not as listed, please notify us at once.

Copy To:

Russ Forba/EPA (1)  
Rich Jackson/MDT (4)  
Keith Large/Montana DEA (1)



---

*Geotechnical Report*

# Geotechnical Report for the Milltown Reservoir Bridge Mitigation Project



Prepared for  
**U.S. Army Corps of Engineers**

December 2006

Prepared by  
**CH2MHILL**  
322 East Front Street, Suite 200  
Boise, Idaho



This report has been prepared under the direction of a Registered Professional Engineer.

Copyright 2006 by CH2M HILL, Inc.

Reproduction in whole or in part without the written consent of CH2M HILL is prohibited.

346017.05.08



CH2M HILL

322 East Front Street

Suite 200

Boise, ID 83702-7359

Tel 208.345.5310

Fax 208.345.5315



**CH2MHILL**

December 19, 2006

346017.05.08

Lynn Daniels, P.E.  
Seattle District Corps of Engineers  
1600 North Ave, W. Ste 105  
Missoula, MT 59807

Subject: Geotechnical Report  
Milltown Bridge Infrastructure Mitigation

Dear Ms. Daniels:

CH2M HILL is pleased to submit the Geotechnical Report for the Milltown Bridge Infrastructure Mitigation Project.

This report includes a summary of the the geotechnical field and laboratory explorations related to bridge mitigation, and a summary of the analyses to date for slope stabilization and foundation underpinning.

The report is intended to represent our final report of the conditions. We acknowledge that we have received additional comments relative to some of the information contained in the report, and it is our intent to respond to those questions in separate correspondence.

We appreciate this opportunity to provide our services to this project.

Sincerely,

CH2M HILL

Dean E. Harris, P.E.  
Geotechnical Engineer

BOI/Report Cover 12\_19\_06.doc

c: Rich Jackson, P.E. \Montana Department of Transportation  
Keith Large \State of Montana DEQ  
Russ Forba, P.E \USEPA



# Contents

---

| Section   | Page      |
|---|-----------|
| <b>1.0 Introduction.....</b>                                    | <b>1</b>  |
| 1.1 Scope of Work.....  | 1         |
| 1.2 Background.....   | 2         |
| 1.2.1 SH 200 Bridge.....  | 2         |
| 1.2.2 I90 Bridges.....  | 2         |
| <b>2.0 Technical Data .....</b>                                 | <b>3</b>  |
| 2.1 Field Exploration.....                                      | 3         |
| 2.1.1 Envirocon Geotechnical Exploration (2005) .....           | 3         |
| 2.1.2 CH2M HILL Spring 2006 Geotechnical Exploration.....       | 7         |
| 2.1.3 Fall 2006 Geotechnical Exploration.....                   | 9         |
| 2.2 Laboratory Testing .....                                    | 10        |
| <b>3.0 Interpretation .....</b>                                 | <b>11</b> |
| 3.1 Geologic Setting.....                                       | 11        |
| 3.1.1 Stratigraphy.....   | 11        |
| 3.1.2 Structure .....   | 11        |
| 3.2 Subsurface Conditions.....                                  | 12        |
| 3.2.1 Embankment Fill .....                                     | 12        |
| 3.2.2 Lacustrine Sediments.....                                 | 19        |
| 3.2.3 SH 200 Bridge, Northwest Side .....                       | 20        |
| 3.2.4 SH 200 Bridge, Southeast Side.....                        | 20        |
| 3.2.5 I90 Bridges, Northwest Side .....                         | 21        |
| 3.2.6 I90 Bridges, Southeast Side .....                         | 21        |
| 3.2.7 Alluvial Sands and Gravels .....                          | 22        |
| 3.2.8 Argillite Bedrock .....                                   | 22        |
| 3.2.9 Type 1 Rock Mass.....                                     | 23        |
| 3.2.10 Type 2 Rock Mass.....                                    | 23        |
| 3.2.11 Distribution of Type 1 and Type 2 Argillite Bedrock..... | 24        |
| 3.3 Groundwater Conditions .....                                | 26        |
| 3.4 Predicted Scour and Blackfoot River Water Surfaces .....    | 27        |
| 3.4.1 Scour Conditions .....                                    | 27        |
| 3.4.2 Blackfoot River Water Surface Elevations .....            | 29        |
| 3.5 Seismicity.....   | 30        |
| 3.5.1 Seismic Parameters.....                                   | 30        |
| 3.5.2 Liquefaction Potential.....                               | 31        |
| <b>4.0 Slope Stability Evaluation.....</b>                      | <b>33</b> |
| 4.1 Soil Properties for Stability Analysis.....                 | 33        |
| 4.1.1 Embankment Fill .....                                     | 33        |
| 4.1.2 Sediment.....   | 34        |



| Section   | Page      |
|---|-----------|
| 4.1.3 Alluvium.....   | 40        |
| 4.1.4 Rock (Argillite) .....  | 41        |
| 4.2 Slope Stability .....   | 41        |
| 4.2.1 Design Requirements.....  | 42        |
| 4.2.2 Stability Analysis for Existing Conditions (Case 1).....            | 42        |
| 4.2.3 Stability Analysis with No Stabilization Measures (Case 2) .....    | 43        |
| 4.2.4 Stability Analysis for Varying Water Levels (Case 3) .....          | 43        |
| 4.2.5 Stability Analysis for Long-Term Conditions (Case 4) .....          | 44        |
| 4.2.6 Stability Analysis for Rapid Drawdown (Case 5).....                 | 44        |
| 4.2.7 Seismic Stability (Case 6).....                                     | 47        |
| 4.2.8 Concluding Remarks on Stability Analysis .....                      | 47        |
| <b>5.0 Embankment Settlement Evaluation.....</b>                          | <b>49</b> |
| 5.1 Settlement of Embankments .....                                       | 49        |
| 5.2 Thickness of Compressible Layers.....                                 | 49        |
| 5.2.1 Preconsolidation Stresses .....                                     | 50        |
| 5.2.2 Estimated Magnitude of Settlement .....                             | 51        |
| 5.2.3 Estimated Duration of Settlement.....                               | 51        |
| <b>6.0 Foundation Evaluation and Recommendations for Mitigation .....</b> | <b>53</b> |
| 6.1 I90 Abutment Evaluation .....   | 53        |
| 6.1.1 Subsurface Profile at the I90 Abutments.....                        | 54        |
| 6.1.2 Subsurface Properties .....   | 54        |
| 6.1.3 Pile Design Parameters.....   | 55        |
| 6.1.4 Concluding Remarks on I90 Abutments.....                            | 58        |
| 6.2 SH 200 Abutment Evaluation .....                                      | 59        |
| 6.2.1 Subsurface Profile at SH 200.....                                   | 60        |
| 6.2.2 Subsurface Properties .....   | 60        |
| 6.2.3 Drag Loads .....  | 61        |
| 6.2.4 Ultimate Resistance Evaluation.....                                 | 62        |
| 6.2.5 Abutment Settlement.....  | 63        |
| 6.2.6 Concluding Remarks on SH 200 Abutments.....                         | 63        |
| 6.3 I90 Pier 3 and SH 200 Pier 3 Evaluation .....                         | 64        |
| 6.3.1 Subsurface Conditions at the Piers .....                            | 64        |
| 6.3.2 Shaft Design Parameters .....                                       | 66        |
| <b>7.0 References.....</b>  | <b>74</b> |
| <b>Appendixes</b>   |           |
| A Boring Logs   |           |
| B Rock Core Photo Logs  |           |
| C Laboratory Tests/Geotechnical Index Parameters                          |           |
| D Prior Stability Analysis for Jet Grout Stabilization                    |           |
| E Section 6 Supporting Materials  |           |

| Tables   | Page |
|--|------|
| 2-1 Borehole Survey Locations and Elevations, 2005 Explorations .....                            | 6    |
| 2-2 Borehole Survey Locations and Elevations, Spring 2006 Explorations .....                     | 8    |
| 2-3 Borehole Survey Locations and Elevations, Fall 2006 Explorations.....                        | 9    |
| 3-1 Estimated Limits of Bedrock Type 1 and Type 2 Elevations.....                                | 25   |
| 3-2 Summary of Groundwater Elevations .....  | 26   |
| 3-3 Summary of 500-Year Pier Scour Calculations .....  | 29   |
| 3-4 Predicted Water Surface Elevations.....  | 29   |
| 3-5 Seismic Design Parameters .....  | 30   |
| 4-1 Index Properties and Direct Shear Results .....  | 35   |
| 4-2 Shear Strength Data from Isotropically Consolidated, Undrained, Triaxial Shear<br>Tests..... | 36   |
| 4-3 Vane Shear Testing Results.....  | 39   |
| 4-4 Fractured Rock Parameters.....   | 41   |
| 4-5 Description of Stability Analysis Cases.....   | 42   |
| 4-6 Stability of Existing Conditions.....  | 43   |
| 4-7 Stability Analysis for Conditions with No Stabilization.....                                 | 43   |
| 4-8 Stability Analysis for Case 3 .....  | 44   |
| 4-9 Factors of Safety for General Scour, Rapid Drawdown Condition.....                           | 46   |
| 5-1 Estimated Values of Maximum Past Vertical Stress ( $\sigma_p'$ ).....                        | 50   |
| 5-2 Estimated Settlement (primary consolidation) .....   | 51   |
| 6-1 Generalized Subsurface Profile .....   | 54   |
| 6-2 Subsurface Properties .....  | 55   |
| 6-3 Drag Load Summary .....  | 57   |
| 6-4 Recommended LPILE Input Parameters .....   | 58   |
| 6-5 Estimated Pile Lengths .....   | 58   |
| 6-6 Generalized Subsurface Profile—SH 200.....   | 60   |
| 6-7 Subsurface Properties .....  | 61   |
| 6-8 SH 200 Drag Load Summary .....   | 62   |
| 6-9 SH 200 Change in Drag Load Summary .....   | 62   |
| 6-10 SH 200 Ultimate Resistance Summary .....  | 63   |
| 6-11 Geometry and Generalized Subsurface Profile.....  | 65   |
| 6-12 Subsurface Properties .....   | 65   |
| 6-13 Argillite Rock Mass Properties.....   | 66   |
| 6-14 Axial Resistance Summary—General Scour Surface.....   | 67   |
| 6-15 Axial Resistance Summary—500-Year Scour Surface .....                                       | 68   |
| 6-16 Uplift Resistance Summary at I90 .....  | 68   |
| 6-17 Axial Resistance Summary at SH 200.....   | 69   |
| 6-18 Uplift Resistance Summary at SH 200.....  | 70   |
| 6-19 Recommended LPILE Input Parameters .....  | 71   |
| 6-20 Estimated Minimum Tip and Shaft Lengths .....   | 72   |



| Figures   | Page |
|---|------|
| 1 Exploration Locations, I90.....   | 4    |
| 2 Exploration Locations, SH 200.....  | 5    |
| 3 Geological Cross Section A, I90 Bridge Embankments and Abutments .....    | 13   |
| 4 Geological Cross Section B, I90 Bridge Embankments and Abutments.....     | 14   |
| 5 Geological Cross Section C, I90 Bridge Embankments and Abutments .....    | 15   |
| 6 Geological Cross Section D, I90 Bridge Embankments and Abutments .....    | 16   |
| 7 Geological Cross Section E, SH 200 Bridge Embankments and Abutments.....  | 17   |
| 8 Geological Cross Section F, SH 200 Bridge Embankments and Abutments ..... | 18   |
| 9 Angle of Internal Friction Versus Relative Density .....                  | 34   |



# 1.0 Introduction

---

This Geotechnical Report summarizes the geotechnical explorations and analyses that have been completed to date for the Milltown Reservoir Bridge Mitigation project. CH2M HILL is designing mitigation measures for Interstate 90 (I90) and State Highway 200 (SH 200) structures that may be affected by drawdown and scour subsequent to the removal of the Milltown Dam as part of remediation activity for the Milltown Reservoir Sediments Site (CERCLA Project). The report includes the following sections:

- Scope of Work: a discussion of the contract scope of work and the background information.
- Technical Data: presents a summary of the field explorations and laboratory testing completed for the project.
- Interpretation: summarizes our interpretations of subsurface conditions.
- Settlement of Embankments: presents a summary of estimated settlement of the embankments at I90 and SH 200 structures.
- Stability of Embankments: summarizes the stability analyses completed for the embankments, with and without stabilization measures.
- Foundation Evaluation and Recommendations: includes a summary of estimated drag loads, and the axial and lateral resistance of foundations at the bridge piers and abutments.

## 1.1 Scope of Work

This work was performed as part of the U.S. Army Corps of Engineers (USACE) Contract No. W912DW-06-1001, Delivery Order (DO) #0002, authorized between CH2M HILL and the USACE on March 23, 2006. This work was completed as part of the overall bridge mitigation design project, covered under DO #0005. CH2M HILL's scope of work includes the following tasks:

1. Geotechnical explorations at the following locations:
  - Stabilization walls at I90 and SH 200 abutment embankments
  - I90 bridge piers
  - Missoula County Pedestrian Bridge
2. Geotechnical evaluation to provide detailed design recommendations. Specific issues considered during our evaluation included:
  - Shear strength and compressibility of the sediment materials
  - Stability of stabilization walls
  - Drag loads on existing and new foundations
  - Axial and lateral capacity of new foundations
3. Preparation of this Geotechnical Report

## **1.2 Background**

CH2M HILL prepared a conceptual design for mitigation measures that was published within the Milltown Bridge Infrastructure Mitigation Report, prepared for the U.S. Environmental Protection Agency (USEPA) and published December 2005. This report identified the following mitigations measures:

### **1.2.1 SH 200 Bridge**

- Underpinning of the central pier (Pier 3) to protect the structure against anticipated scour.
- Construction of a temporary wall near the base of the abutment slope to increase the stability of the slopes during drawdown.

### **1.2.2 I90 Bridges**

- Abutment underpinning for each structure to protect against settlement caused by drawdown of the reservoir.
- Underpinning of the central pier (Pier 3) of each bridge to protect the structures against anticipated scour.
- Construction of a temporary wall near the base of the abutment slope to increase the stability of the slopes during drawdown.

The Mitigation Report was reviewed by the Montana Department of Transportation, the owner of the bridges. Subsequent to this review, additional evaluation was completed to consider abutment underpinning on each of the structures.

During design of the mitigation measures, CH2M HILL determined that, in addition to increased scour, there is a possibility that movement of the Blackfoot River thalweg could further threaten the abutments of the I90 and SH 200 bridges. Therefore, it was determined that permanent stabilization and scour protection measures are necessary.



## 2.0 Technical Data

---

### 2.1 Field Exploration

Several stages of geotechnical explorations have been performed to provide subsurface data for the infrastructure mitigation efforts. These are summarized as follows:

- Envirocon Geotechnical Exploration (2005)
- CH2M HILL Spring 2006 Geotechnical Exploration
- CH2M HILL Fall 2006 Geotechnical Exploration

These exploration programs are discussed separately in the following sections of this report.

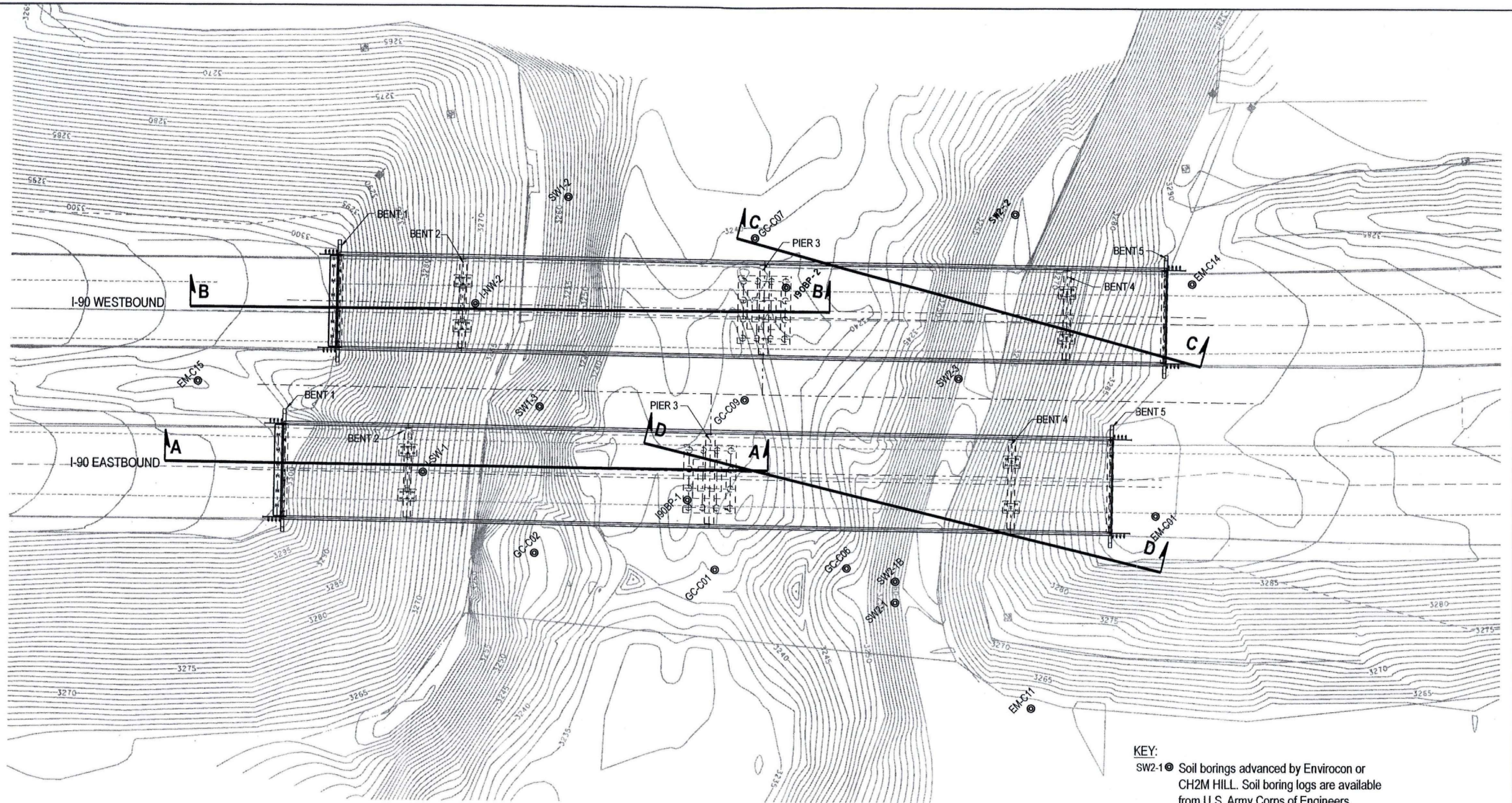
#### 2.1.1 Envirocon Geotechnical Exploration (2005)

During 2005, Envirocon, based in Bozeman, Montana, performed geotechnical explorations to support the infrastructure mitigation measures and remediation design. The explorations included soil borings advanced from a barge within the reservoir, and borings advanced adjacent to the bridges and interstate using track- and truck-mounted drilling equipment. Borings were logged by EMC<sup>2</sup>. Final boring logs were prepared by EMC<sup>2</sup>, and are included in Appendix A.

Twenty-four of the soil borings advanced during the 2005 exploration program were used as part of our evaluation, and are summarized in Table 2-1. Figures 1 and 2 shows the locations of the soil 2005 borings that were performed in the vicinity of the bridges. Results of the drilling program are presented in the Remedial Design Data Summary Report #3 (Envirocon, 2005).

Samples collected from the drilling activities were used in a laboratory testing program that included index testing, as well as strength and compressibility testing. A summary of the sampling program and laboratory test results was provided by Envirocon in the Remedial Design Data Summary Report #3 (Envirocon, 2005).



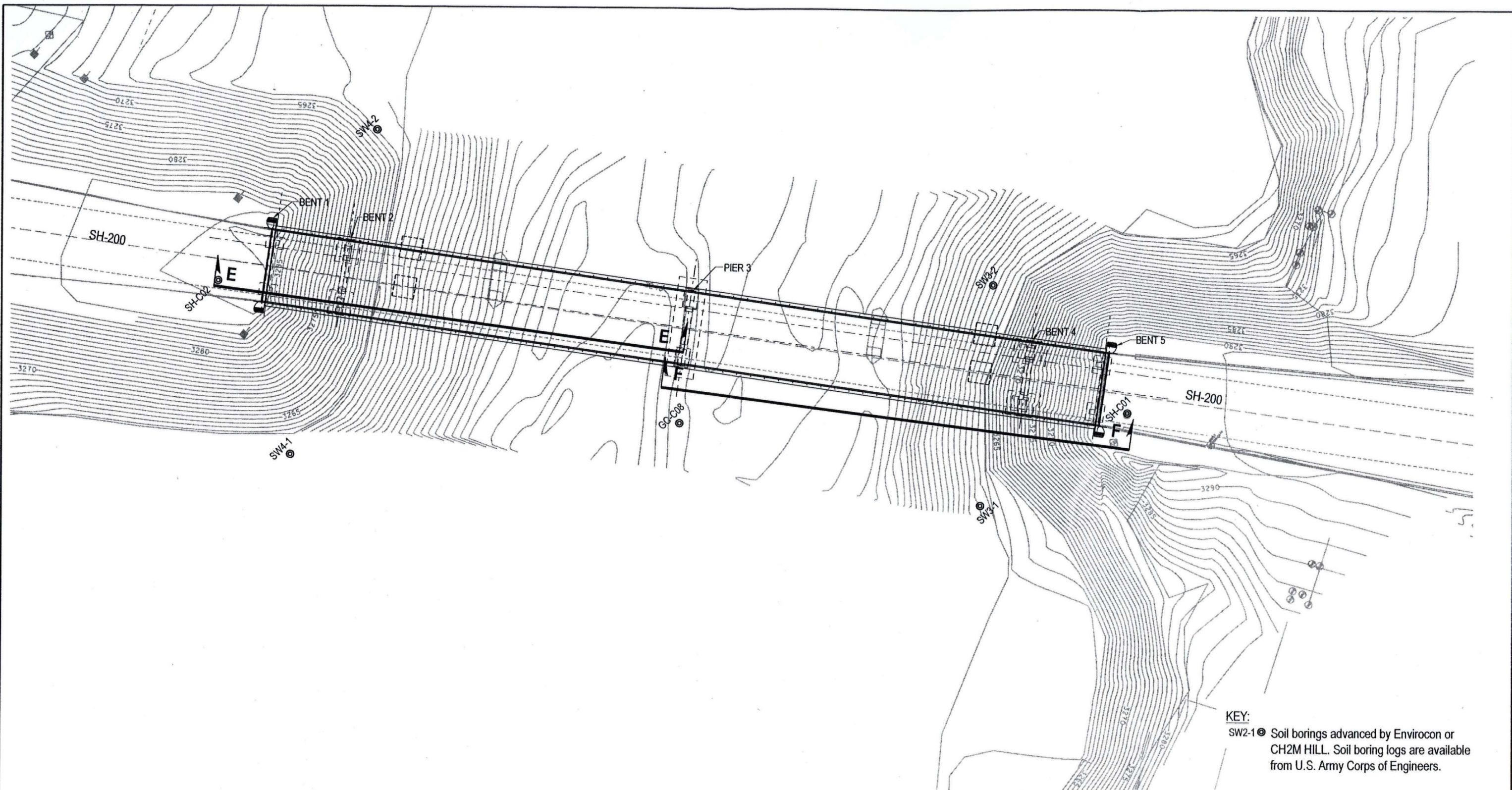


KEY:  
 SW2-1● Soil borings advanced by Envirocon or  
 CH2M HILL. Soil boring logs are available  
 from U.S. Army Corps of Engineers.

20 0 40  
 Scale: 1"=40'

MILLTOWN BRIDGE INFRASTRUCTURE  
 MITIGATION  
 SLOPE STABILIZATION  
 FIGURE 1  
 EXPLORATION LOCATIONS,  
 I-90





20 0 40  
 Scale: 1"=40'

MILLTOWN BRIDGE INFRASTRUCTURE  
 MITIGATION  
 SLOPE STABILIZATION

FIGURE 2  
 EXPLORATION LOCATIONS,  
 SH-200



**TABLE 2-1**  
Borehole Survey Locations and Elevations, 2005 Explorations

| Boring ID          | Northing<br>(feet) | Easting<br>(feet) | Ground Surface Elevation<br>(feet) | Total Depth<br>(feet) |
|--------------------|--------------------|-------------------|------------------------------------|-----------------------|
| EM-C01             | 17043672.1         | 918748            | 3290.6                             | 65.0                  |
| EM-C02             | 17043173.9         | 919275.2          | 3279.5                             | 55.0                  |
| EM-C03             | 17042950.6         | 919597.4          | 3280.9                             | 65.5                  |
| EM-C04             | 17042763.1         | 919878.4          | 3285.0                             | 60.0                  |
| EM-C05             | 17042437.9         | 920357.6          | 3292.4                             | 57.5                  |
| EM-C06             | 17043113.5         | 919241.1          | 3261.4                             | 41.0                  |
| EM-C07             | 17042704.9         | 919847.4          | 3262.6                             | 35.5                  |
| EM-C08             | 17043407.2         | 918892.8          | 3262.6                             | 40.0                  |
| EM-C09             | 17042900.8         | 919557.2          | 3261.8                             | 45.0                  |
| EM-C10             | 17042333.3         | 920361.7          | 3261.6                             | 30.5                  |
| EM-C11             | 17043658.8         | 918654.6          | 3261.5                             | 35.0                  |
| EM-C12             | 17042807.3         | 919904.2          | 3282.6                             | 66.0                  |
| EM-C14             | 17043723.7         | 918829.7          | 3290.2                             | 69.0                  |
| EM-C15             | 17044007.4         | 918526.7          | 3299.7                             | 77.0                  |
| EM-C17 and EM-C17B | 17044375.1         | 918208            | 3310.6                             | 90.0                  |
| EM-C21             | 17044093.4         | 918455.5          | 3302.8                             | 76.5                  |
| SH-C01             | 17044064           | 919556.8          | 3291.0                             | 94.5                  |
| SH-C02             | 17044389.3         | 919344.2          | 3287.3                             | 94.0                  |
| GC-C01             | 918610.4           | 17043795.4        | 3283.3                             | 35.5                  |
| GC-C02             | 918565.9           | 17043856.2        | 3243.4                             | 43.0                  |
| GC-C06             | 918647.3           | 17043754.4        | 3249.5                             | 49.0                  |
| GC-C07             | 17043872.8         | 918723.9          | 3239.3                             | 72.5                  |
| GC-C08             | 17044203.8         | 919428.2          | 3237.8                             | 33.5                  |
| GC-C09             | 17043832           | 918671            | 3238.4                             | 65.0                  |

**NOTES:**

<sup>1</sup>Horizontal Datum-UTM 12 international feet.

<sup>2</sup>Vertical Datum-NAVD88.

<sup>3</sup>Field work by Roger Austin, PLS, on August 10, 2005.

<sup>4</sup>EM-C17 was terminated at 60 feet below the surface and redrilled 5 feet east as EM-C17B to a depth of 90 feet.

<sup>5</sup>GC-C09 northing, easting, and elevation are estimated based on proposed location coordinates, typical reservoir/deck elevations, and measured distance from barge deck to the top of sediments. GPS survey readings of actual location coordinates were not possible due to bridge interference with communication between survey equipment and satellites.



### 2.1.2 CH2M HILL Spring 2006 Geotechnical Exploration

During spring 2006, additional geotechnical explorations were conducted to gain additional subsurface geotechnical information to support design of the mitigation measures identified in the Milltown Bridge Infrastructure Mitigation Report (CH2M HILL, 2005) and for use by others in evaluation of the Missoula County Pedestrian Bridge. Additional information was needed in order to design mitigation measures to protect the infrastructure at the Milltown Dam reservoir, as the pool is drawn down and the dam is removed.

The scope of work was completed in two phases. The first phase included borings advanced using a track-mounted drill rig, at locations accessible from the shore. The first phase of work was completed by Haz Tech Drilling, Inc., of Meridian, Idaho. The second phase included borings advanced from a barge set up in the reservoir pool. The second phase of work was completed by Crux Subsurface, Inc., of Spokane, Washington.

Both phases of work required coordination with NorthWestern Energy, the operators of Milltown Dam, to control the reservoir pool elevation during the exploration. For the first phase of work, the reservoir pool was drawn down approximately 2 feet (to approximate elevation 3258 feet); for the second phase of work the pool was maintained at approximate elevation 3260 feet.

#### 2.1.2.1 Exploration Summary

The original scope of work included 14 borings to be advanced at the project site. This included:

- Two borings along the toe of the I90 embankment, west of the west abutments (EB-1 and EB-2)
- Four borings at the stabilization wall locations for the I90 bridges (SW1-1, SW1-2, SW2-1, and SW2-2)
- Two borings at the I90 Pier 3 locations (I90BP-1 and I90BP-2)
- Four borings at the SH 200 stabilization wall locations (SW3-1, SW3-2, SW4-1, and SW4-2)
- Two borings at the abutments of the Missoula County Pedestrian Bridge (PB-1 and PB-2)

Borings EB-1, EB-2, SW1-1, SW4-1, SW4-2, and PB-1 were completed between March 23 and March 31. During the second phase of work, which was completed between April 11 and April 29, the remaining borings in the scope were completed (borings SW1-2, SW2-1, SW2-2, I90BP-1, I90BP-2, SW3-1, SW3-2, and PB-2), plus three additional shallow borings (SW1-3, SW2-1B, and SW2-3) that were advanced to collect additional sample material in key locations without any previous subsurface information. The locations of the spring 2006 soil borings are shown in Figures 1 and 2. The borings are summarized in Table 2-2.

Track-rig-based boreholes were advanced with hollow-stem auger and mud rotary drilling techniques, using a CME 850 track-mounted drill rig. All barge holes were advanced using mud rotary techniques with a tricone bit and casing advancement, with a Burley 4500C drill mounted on a 30-foot aluminum barge. During both phases of work, HQ-sized triple-tube rock coring techniques were used when advancement in the alluvium was too slow, or when argillite was encountered. All boreholes were abandoned and backfilled with bentonite pellets up to the ground surface.



**TABLE 2-2**  
Borehole Survey Locations and Elevations, Spring 2006 Explorations

| Boring I.D. | Northing    | Easting     | Elevation (ft) | Depth (ft, bgs) | Description  |
|-------------|-------------|-------------|----------------|-----------------|--|
| EB-1        | 986993.2200 | 871911.0000 | 3267.6         | 55.5            | HSA and Mud Rotary; Located near toe of I90 embankment, west of Blackfoot River                          |
| EB-2        | 986643.9300 | 872134.1900 | 3261.2         | 42.0            | HSA and Mud Rotary/HQ Triple-tube Rock Core; Located near toe of I90 embankment, west of Blackfoot River |
| I90 BP-1    | 986498.6325 | 872450.0925 | 3237.7         | 50.1            | Mud Rotary/HQ Triple-tube Rock Core; Located at I90 Bridge Pier 3, advanced through footing seal         |
| I90 BP-2    | 986523.5657 | 872543.4647 | 3235.1         | 50.0            | Mud Rotary/HQ Triple-tube Rock Core; Located at I90 Bridge Pier 3, advanced through footing seal         |
| PB-1        | 987131.8208 | 873464.4666 | 3262.9         | 31.5            | HSA and Mud Rotary; Located at Pedestrian Bridge abutments   |
| PB-2        | 986817.7979 | 873561.2062 | 3255.5         | 27.0            | Mud Rotary; Located at Pedestrian Bridge abutments   |
| SW1-1       | 986526.9600 | 872244.0500 | 3261.5         | 41.4            | HSA and Mud Rotary; Located at stabilization wall, I90 west abutment slope                               |
| SW1-2       | 986616.8289 | 872513.0745 | 3252.0         | 42.0            | Mud Rotary/HQ Triple-tube Rock Core; Located at stabilization wall, I90 west abutment slope              |
| SW1-3       | 986570.1185 | 872439.5938 | 3246.5         | 19.0            | Mud Rotary/HQ Triple-tube Rock Core; Located at stabilization wall, I90 west abutment slope              |
| SW2-1       | 986405.1389 | 872473.9968 | 3248.9         | 34.0            | Mud Rotary/HQ Triple-tube Rock Core; Located at stabilization wall, I90 east abutment slope              |
| SW2-1B      | 986410.7325 | 872480.6240 | 3250.0         | 12.5            | Mud Rotary; Located at stabilization wall, I90 east abutment slope                                       |
| SW2-2       | 986470.1849 | 872627.7661 | 3252.1         | 50.5            | Mud Rotary/HQ Triple-tube Rock Core; Located at stabilization wall, I90 east abutment slope              |
| SW2-3       | 986444.5314 | 872561.0625 | 3248.5         | 10.5            | Mud Rotary; Located at stabilization wall, I90 east abutment slope                                       |
| SW3-1       | 986744.0536 | 873316.6862 | 3254.5         | 40.5            | Mud Rotary/HQ Triple-tube Rock Core; Located at stabilization wall, SH 200 east abutment slope           |
| SW3-2       | 986799.5519 | 873390.7458 | 3251.9         | 38.5            | Mud Rotary/HQ Triple-tube Rock Core; Located at stabilization wall, SH 200 east abutment slope           |
| SW4-1       | 986980.4732 | 873144.2740 | 3261.2         | 41.5            | HSA and Mud Rotary; Located at stabilization wall, SH 200 west abutment slope                            |
| SW4-2       | 987040.2440 | 873271.5401 | 3262.0         | 41.3            | HSA and Mud Rotary; Located at stabilization wall, SH 200 west abutment slope                            |

Note: All coordinates and elevations are based on the North American Vertical Datum, NAVD 1988.

### 2.1.3 Fall 2006 Geotechnical Exploration

During fall 2006, additional geotechnical explorations were performed to gain additional geotechnical information along the slopes at the I90 abutments, install inclinometers in the I90 abutments, and to core jet grout test columns.

Inclinometer installation and jet grout test column coring was performed by Ruen Drilling, Inc. of Clark Fork, Idaho. The original scope of work included the installation of four inclinometers: two each at Bent No. 2 (on the west bank of the Blackfoot River) and Bent No. 4 (on the east bank). However, due to limited height access and the presence of tension cracks and unstable slopes on the east work platform, no inclinometers were installed on the east side of the Blackfoot River at Bent No. 4.

The findings from coring of jet grout test columns will be presented in a separate memorandum.

#### 2.1.3.1 Exploration Summary

Inclinometers I-SW-1 and I-NW-2 were installed on November 1 and November 7, 2006, respectively. Inclinometer I-SW-1 is centered between the existing pile caps at Bent No. 2, I90 eastbound bridge, and I-NW-2 is centered between the existing pile caps at Bent No. 2, I90 westbound bridge. The inclinometer casing was installed within vertical boreholes advanced from the existing temporary work platforms. Additional inclinometer casing was provided to accommodate future extensions to reach the finished slope face for long-term monitoring.

Because of limited access below the I90 bridges, primarily at Bent No. 4 on the east bank, a CME 45 sled-mounted drill rig was initially mobilized by Ruen Drilling, Inc. However, because of difficult drilling through the gravels and cobbles of the upper embankment fill layer, Ruen Drilling mobilized a second drill rig, a CME 850 track-mounted drill rig. The CME 850 track-mounted drill rig was then used to complete all of the boreholes. The inclinometer boreholes were advanced using mud-rotary techniques with a tricone bit and HWT casing advancement to refusal within the alluvium layer. Upon refusal, HQ-sized triple-tube rock coring was utilized to advance the borehole into the argillite bedrock.

Figure 1 shows the locations of the Fall 2006 inclinometer borings. These borings are summarized in Table 2-3.

TABLE 2-3  
Borehole Survey Locations and Elevations, Fall 2006 Explorations

| Borehole/Jet<br>Grout Test<br>Column ID | Drill<br>Location<br>ID | Approximate<br>Elevation<br>(ft) | Termination<br>Depth<br>(ft bgs) | Description                                | Date<br>Completed |
|---|-------------------------|----------------------------------|----------------------------------|--|-------------------|
| I-SW-1                                  | --                      | 3264.5                           | 48.5                             | Mud rotary and HQ-size triple-tube coring. | 11/1/06           |
| I-NW-2                                  | --                      | 3264.5                           | 50.0                             | Mud rotary and HQ-size triple-tube coring. | 11/7/06           |



For both the spring and fall 2006 explorations, a CH2M HILL geotechnical engineer or geologist observed drilling activities and maintained written logs, including a record of drilling conditions, sample descriptions, and relative descriptions of jet grout test column quality. Soil samples were examined in the field and visually classified in general accordance with ASTM D2488—Standard Practice for Description and Identification of Soils (Visual-Manual Procedure).

Standard penetration tests (SPT) were conducted with a standard 2-inch O.D. split-spoon sampler, in general accordance with ASTM D1586—Standard Test Method for Penetration Test and Split-Barrel Sampling of Soils. Disturbed soil samples were visually inspected and collected from the split-spoon sampler. Periodically, a 3-inch O.D. Dames & Moore split-barrel sampler was used alternatively, in order to attempt better recovery in coarse-grained material. A hydraulic trip-hammer, with a 140-lb hammer free-falling 30 inches, was used to drive the samplers. The number of blows to drive the sampler for each 6-inch increment of an 18-inch drive was recorded on the boring logs. The sum of the blows for the last 12 inches of penetration, or fraction of, is recorded as the standard penetration resistance, or N-Value. After the sampler was driven and the blow counts were recorded, the sampler was withdrawn from the borehole for recovery of the disturbed soil sample. Disturbed soil samples were logged and placed in plastic bags.

Rock coring was completed using a triple-tube coring system to collect HQ-size core samples. Rock Quality Designation (RQD) and a rock strength, or hardness, were measured for each rock core sample recovered. The RQD is calculated as the ratio of the sum of the length of rock core fragments longer than 4 inches to the total drilled footage for that run, expressed as a percentage. Rock core was classified and inspected, then placed in core boxes for storage. Each core box was photographed and included in a rock core photographic log in Appendix B. Photographs of rock core taken by others are included in the report prepared by Envirocon, titled *Remedial Design Data Summary Report No. 3: Covering November 2004 Through August 2005 Field Activities*, and dated November 8, 2005.

## 2.2 Laboratory Testing

Laboratory testing for the project has been completed by Envirocon, during the exploration activities that were described previously, and by CH2M HILL, using samples recovered from explorations performed under our observation, as described previously.

The findings from the Envirocon laboratory testing were presented in the Remedial Design Data Summary Report (Envirocon, 2006).

The findings from laboratory testing performed under authorization by CH2M HILL are included in Appendix C. A table summarizing the geotechnical index parameters from Envirocon and CH2M HILL is also included in Appendix C. Discussions of compressibility and strength parameters from the testing are presented in the appropriate sections that discuss embankment settlement, embankment stability, or pile foundations.



## 3.0 Interpretation

---

### 3.1 Geologic Setting

The local geologic setting is summarized from Berg (2006). The geology in the project vicinity consists primarily of Precambrian-age bedrock that forms the mountains, and Quaternary-age unconsolidated deposits filling the valleys.

#### 3.1.1 Stratigraphy

The bedrock in the vicinity of the site belongs to the Belt Supergroup, which consists of metasedimentary rocks including siltite, argillite, and quartzite. The bedrock in the immediate project vicinity includes the Bonner and Mount Shields Formations of the Belt Supergroup. The Bonner Formation is described as "generally massive beds of pink to tan arkosic quartzite with sparse argillite beds." The Mount Shields Formation is described as "reddish quartzite and subordinate argillite and siltite in the lower and middle parts, with predominantly reddish argillite in the upper part." The argillite includes abundant planar laminations and ripple cross-laminations.

The unconsolidated deposits in the project vicinity include glacial lake deposits, alluvial terrace deposits, and alluvial deposits of modern channels and floodplains. Glacial lake deposits in the vicinity include varved (laminated) fine-grained deposits with lenses of fine quartzite gravels. Alluvial terrace deposits consist of gravelly deposits, and form flat surfaces 10 to 20 feet above the alluvial deposits. The alluvial deposits include rounded gravel, sand, silt, and clay along the Clark Fork and Blackfoot Rivers. The predominant rock type in the alluvium is resistant quartzite derived from the Belt Supergroup. After construction of the Milltown Dam, lacustrine sediments were deposited in Milltown Reservoir during large flood events. The lacustrine sediments consist of interbedded fine sands, silts, and clays. The alluvial deposits and lacustrine sediments are described in more detail under Section 3.2 Subsurface Conditions.

#### 3.1.2 Structure

The Clark Fork River valley flows along the Lewis and Clark line, which is a major shear zone that extends from eastern Idaho to Helena, Montana. Movement along faults in this zone began in the Middle Proterozoic and continued into the Holocene. The trace of this fault in the project vicinity is evidenced by deformed rocks on both sides of the Clark Fork valley; but the actual fault trace is obscured by younger deposits. Thrust faults of Laramide age along which northern and northeastward transport has occurred are important structural features on the Clark Fork valley.

The bedrock in the project vicinity has been deformed by folding and faulting. Based on the geologic map by Berg (2006), the bedding in the project vicinity dips to the northwest, southeast, and southwest with angles that range from 18 to 53 degrees. In addition, overturned bedding that dips at an angle of 70 degrees is mapped on the north side of the



Blackfoot River; which indicates the high degree of deformation of the bedrock in the project vicinity. Other structural features in the project vicinity include jointing in the argillite.

## **3.2 Subsurface Conditions**

The subsurface explorations have identified four major stratigraphic units within the project limits. These include:

- Man-made embankment fill
- Lacustrine sediments deposited in Milltown Reservoir
- Alluvial sands and gravels deposited by the Clark Fork and Blackfoot Rivers
- Argillite bedrock

Because the thickness and composition of these units varies significantly, six geologic cross sections were prepared. The locations of the geologic cross sections are shown in Figures 1 and 2. Figures 3 through 6 show geologic cross sections at the I90 bridge embankments and abutments. Figures 7 and 8 show geologic cross sections in the vicinity of the SH 200 bridge embankments and abutments.

Each of the stratigraphic units is described in greater detail as follows.

### **3.2.1 Embankment Fill**

The embankment fill material consists primarily of gravelly material used to construct roadway and bridge approach embankments for SH 200 and I90. It is not known if the embankments were constructed of borrow material, or if the embankments were constructed from material from other highway cuts in the near vicinity.

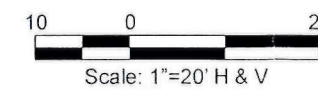
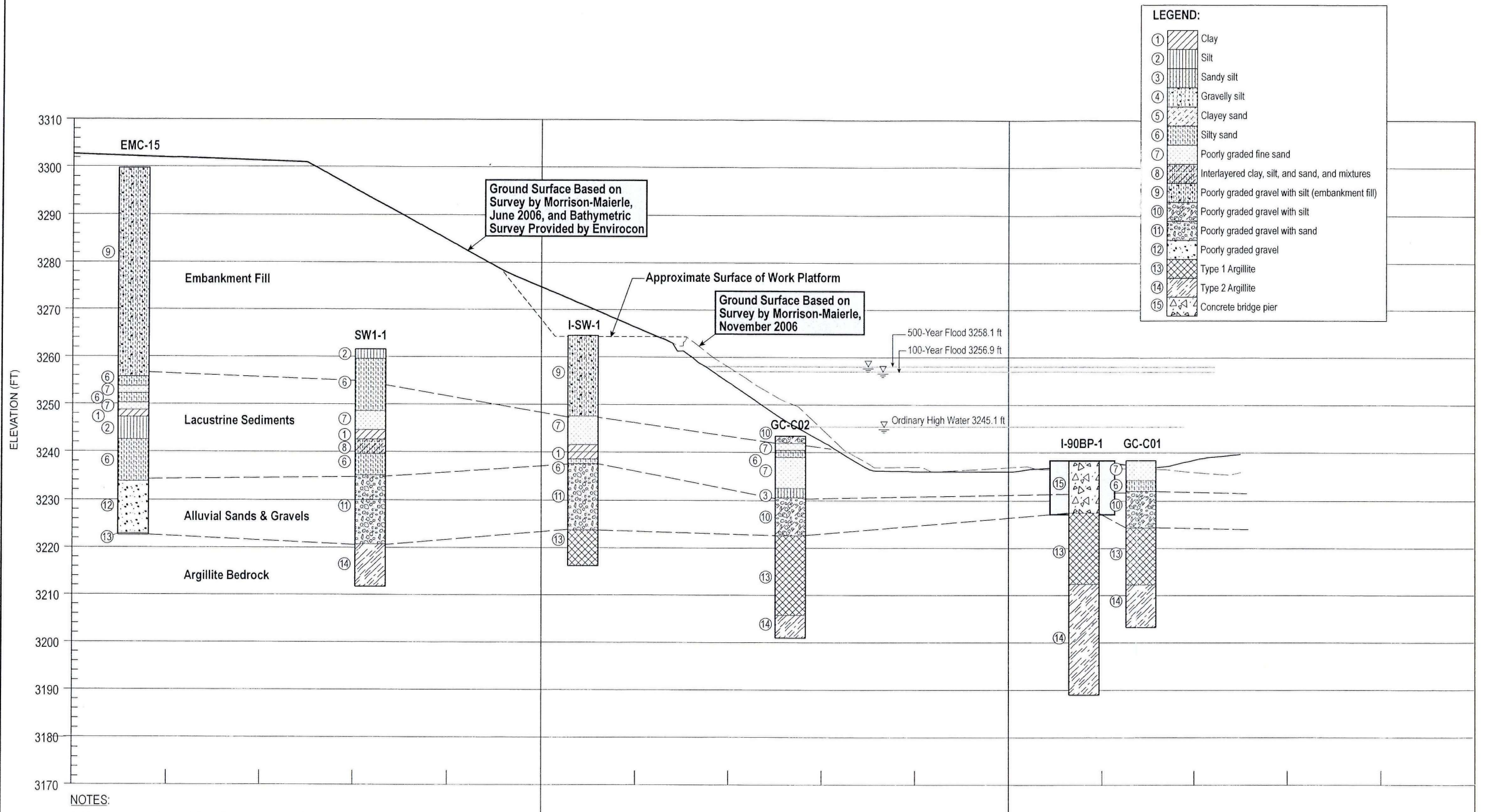
The embankment fills for each structure were constructed above the reservoir sediments at the edges of the Blackfoot River, and the thickness of the fill varies from the toe of slope to the top of the embankment. Based on soil boring information, the fill material is typically described as brown, moist, poorly graded gravel with sand and silt. The gravels are multi-colored, multiple lithologies, and range from rounded to broken and fractured. Cobble-sized gravels were exposed on the fill slopes. SPT N-values in this material ranged from six blows per foot (bpf) to "refusal" (more than 50/blows for 6 inches). For sandy materials, these N-values would typically be considered to indicate loose to very dense conditions. However, because the gravels and cobble are often larger than the Standard SPT sampler, very high N-values should not be assumed to represent very dense conditions for the embankment fill.

More detailed discussions are provided for each of the structures in the following paragraphs.

#### **3.2.1.1 SH 200 Bridge**

The SH 200 embankments were constructed in 1949. The boring logs indicate that the materials used in the embankments include gravel with sand, gravel with silt and sand, and gravel with clay and sand. N-values indicate that the embankment material is at a wide range of relative densities. However, it should be noted that some of the SPTs were driven into cobbly material, and thus the high N-values may not truly represent high relative density. For example, in SH-C02 the logger noted that in multiple samples the sampler was "bouncing on a cobble."

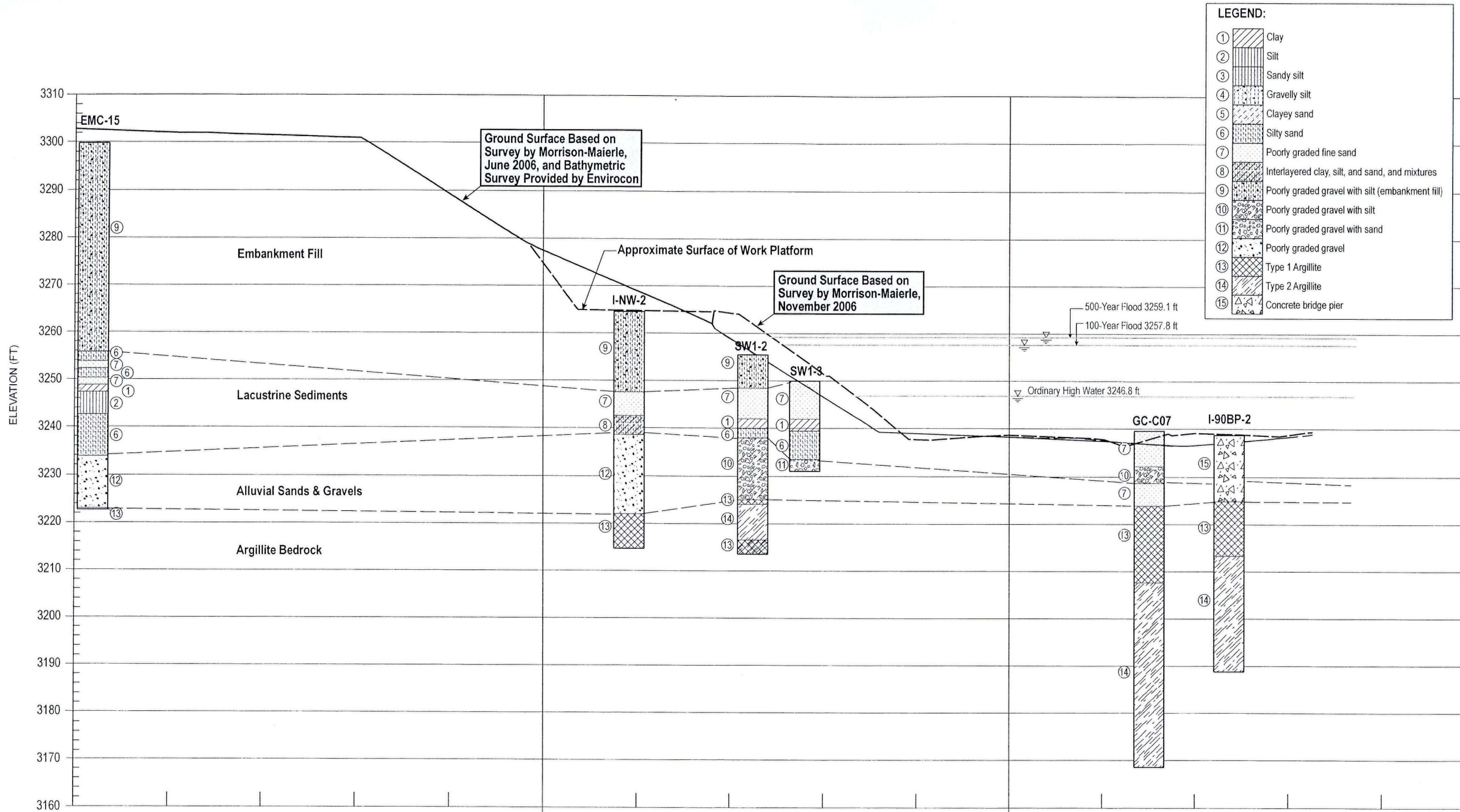




MILLTOWN BRIDGE INFRASTRUCTURE  
MITIGATION  
SLOPE STABILIZATION

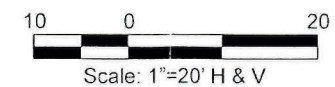
FIGURE 3  
GEOLOGIC CROSS SECTION  
SECTION A  
I-90 EB





**NOTES:**

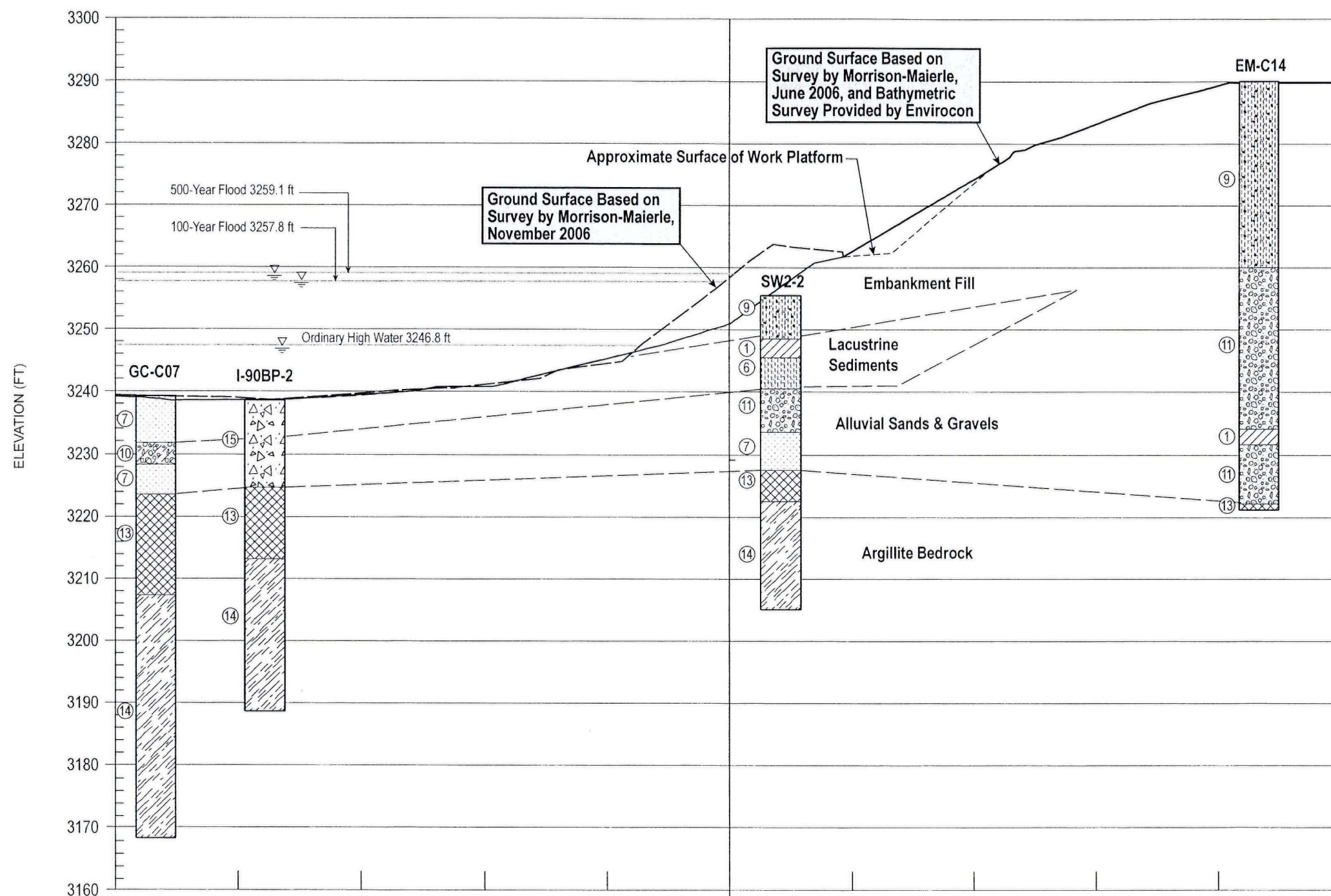
1. Borings are not located directly on section cut line.
3. The layering shown is based on soil borings that included sampling at discrete intervals. Therefore in some cases the material type present between samples is unknown. These symbolic logs represent CH2M HILL's opinion of the conditions.
4. The lines representing divisions between the different soil and rock units are approximate and it is likely that the actual conditions will vary.



MILLTOWN BRIDGE INFRASTRUCTURE  
MITIGATION  
SLOPE STABILIZATION

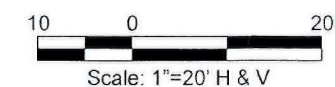
**FIGURE 4**  
**GEOLOGIC CROSS SECTION**  
**SECTION B**  
**I-90 WB**





**NOTES:**

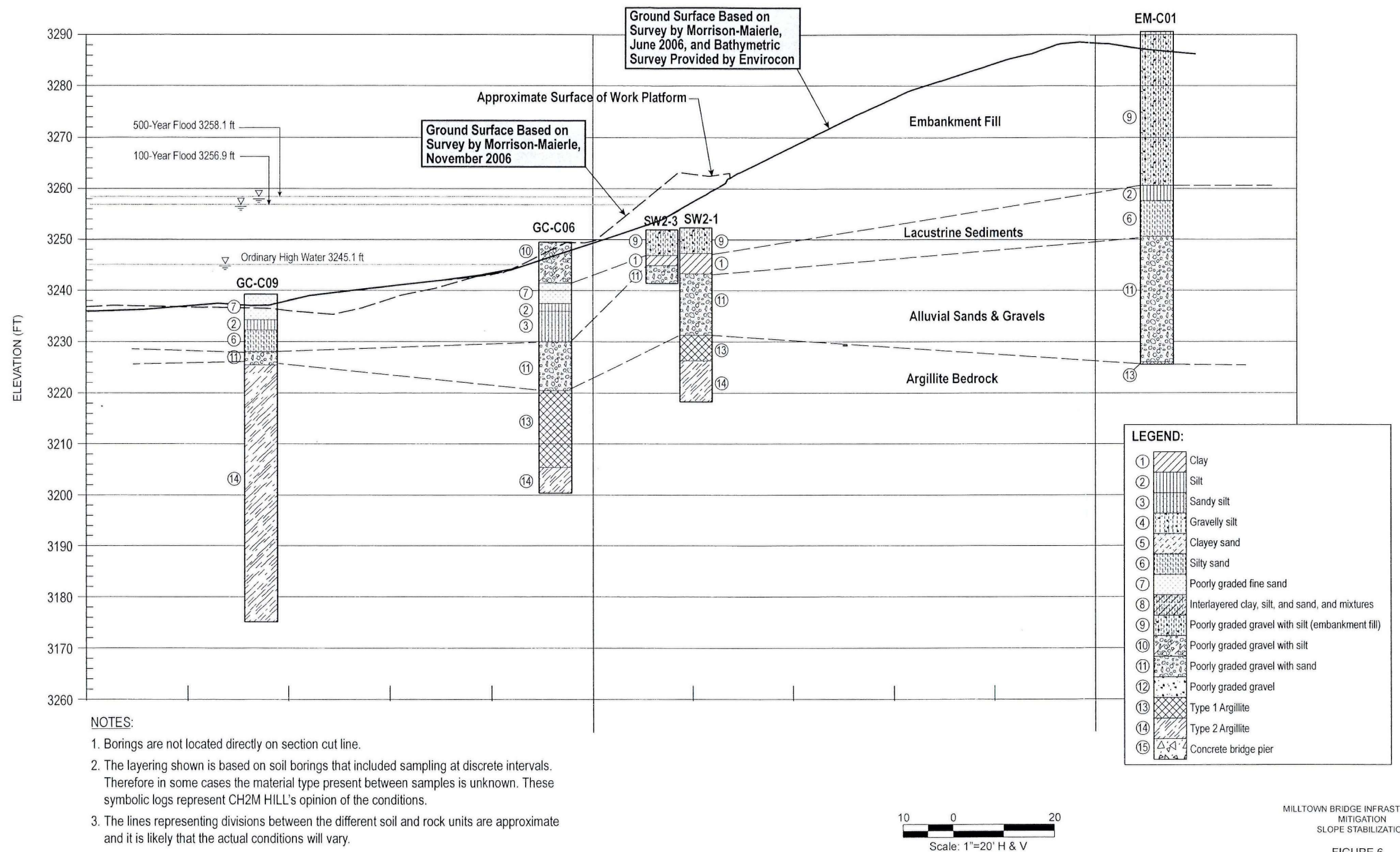
1. Borings are not located directly on section cut line.
2. The layering shown is based on soil borings that included sampling at discrete intervals. Therefore in some cases the material type present between samples is unknown. These symbolic logs represent CH2M HILL's opinion of the conditions.
3. The lines representing divisions between the different soil and rock units are approximate and it is likely that the actual conditions will vary.



MILLTOWN BRIDGE INFRASTRUCTURE  
MITIGATION  
SLOPE STABILIZATION

FIGURE 5  
GEOLOGIC CROSS SECTION  
SECTION C  
I-90

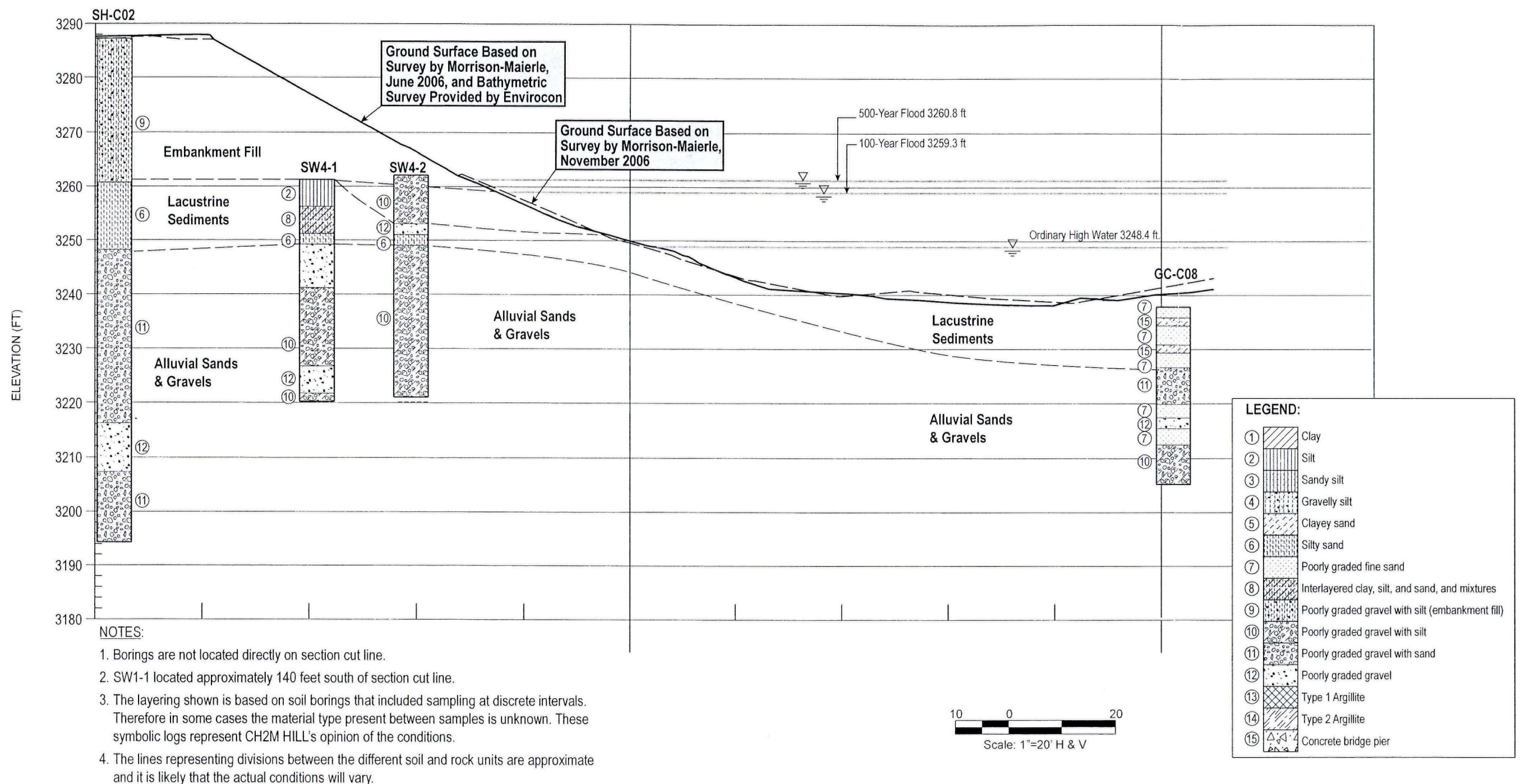




MILLTOWN BRIDGE INFRASTRUCTURE  
MITIGATION  
SLOPE STABILIZATION

FIGURE 6  
GEOLOGIC CROSS SECTION  
SECTION D  
I-90 EB

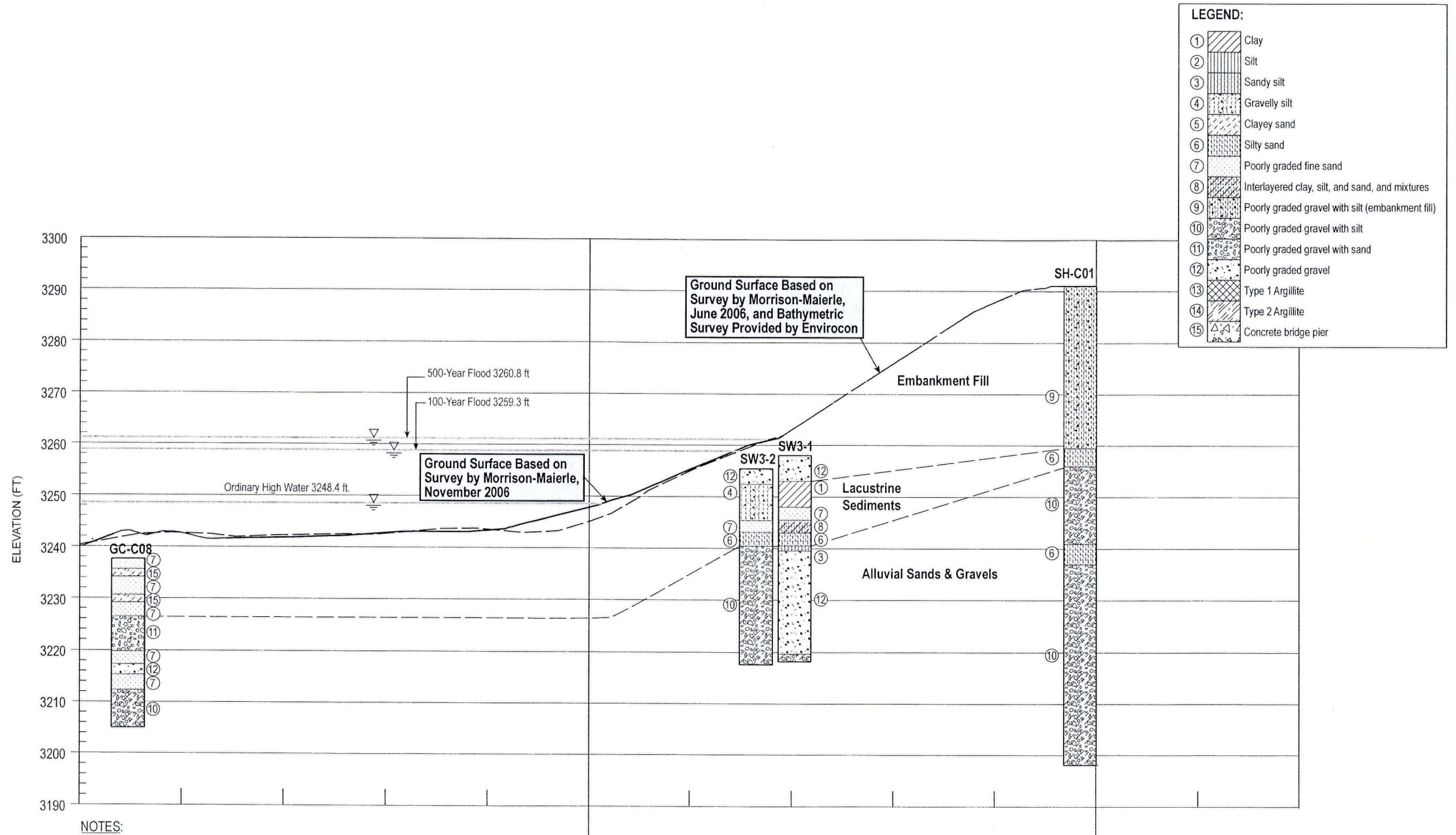




MILLTOWN BRIDGE INFRASTRUCTURE  
MITIGATION  
SLOPE STABILIZATION

FIGURE 7  
GEOLOGIC CROSS SECTION  
SECTION E SH-200





MILLTOWN BRIDGE INFRASTRUCTURE  
MITIGATION  
SLOPE STABILIZATION

**FIGURE 8**  
**GEOLOGIC CROSS SECTION**  
**SECTION F SH-200**



### **Northwest Side**

Boring SH-C02 was drilled through the northwest approach embankment of the SH 200 Bridge. The embankment fill is up to 35 feet in thickness at this location, and is described primarily as gray to brown, poorly graded gravel with silt and sand. SPT N-values in this embankment range from seven bpf to 100 blows for less than 1 foot. These values indicate loose to very dense material, and overall a high variability in the relative density of the embankment fill. The N-values were much higher in the upper 10 feet of embankment versus the lower 25 feet of the fill.

### **Southeast Side**

Boring SH-C01 was drilled through the southeast approach embankment of the SH 200 bridge. The embankment fill is up to 36.5 feet in thickness and is described primarily as gray to brown, poorly graded gravel with sand to gravel with clay and sand. Blow counts in the embankment fill range from 9 to 67 bpf, which indicates medium-dense to very dense gravels. The drill logs noted varying auger rates throughout the embankment. Based on N-values, the upper 5 feet of the embankment may be higher relative density than the lower 30 feet.

### **3.2.1.2 I90 Bridges**

The I90 embankments were constructed in 1964. The boring logs indicate that the materials used in the embankments generally include gravel with sand, gravel with silt and sand, and sand with silt and gravel. The N-values indicate that the embankment material is at a wide range of relative densities. However, it should be noted that some of the SPTs were driven into cobbly material, and thus the high N-values may not truly represent high relative density. The boring logs noted several intervals of "drilling through cobbles."

### **Northwest Side**

Boring EM-C15 was drilled through the northwest approach embankment of the I90 bridges. The embankment fill is up to 44 feet in thickness at this location and is described primarily as gray to brown, poorly graded gravel with sand. SPT N-values in the embankment fill range from 11 to 100 bpf. Because of the presence of gravel, CH2M HILL interprets these N-values to indicate medium-dense conditions. The drilling log indicates drilling through gravels and boulders.

### **Southeast Side**

Borings EM-C14 and EM-C01 were drilled through the southeast approach embankments of the I90 bridges. The embankment fill is up to 38.5 feet in thickness at this location and is described primarily as gray to brown, poorly graded gravel with sand and silty gravel, although sandy layers were encountered in both borings in this embankment. SPT N-values in the embankment fill range from 13 to 100 blows for less than 1 foot. Because of the presence of gravel, CH2M HILL interprets these N-values to indicate medium-dense conditions. The drilling log indicates drilling through gravels and boulders.

### **3.2.2 Lacustrine Sediments**

Lacustrine sediments were deposited within the slack-water Milltown Reservoir pool. Much of the material was probably deposited in 1908, soon after completion of the dam. The sediments were typically deposited on the existing alluvial gravels that underlie the Blackfoot River and Clark Fork River floodplains and channels. These sediments within the



project limits include interbedded, stratified layers and lenses of clay, silt, sand, and gravel, and thinly interbedded mixtures of these materials. Woody debris and organic materials were also observed in samples from this unit.

The lacustrine sediments observed in the borings range from approximately 3 to 27 feet in thickness throughout the project area. The top elevation of the sediments is approximately 3261 feet, which corresponds with deposition in full pool conditions. In some areas, such as the Blackfoot River channel, the uppermost portions of the sediments are absent and may have been scoured by currents. The bottom elevation of sediments (contact of sediment with alluvium) varies based on the original configuration of the alluvium upon which the sediments were deposited, and in general ranges from approximately 3226 to 3250 feet in elevation, based on information from the boring logs.

Although the sediment unit is highly variable, the soil borings indicate that the predominant materials consist of fine sand, silty sand, and sandy silt, with interbedded silt, clay, and organic debris. The silt and clay layers range in thickness from less than 1 inch to several feet.

The silty sands are described as primarily poorly graded, brown to gray, wet, loose, and fine grained. The sandy silts are described as primarily brown, gray to dark-gray, wet, soft to stiff, and non-plastic to low plasticity. Layers of gray silt, medium-plasticity clay, and organic silts and sands were observed within the sediments in some of the borings.

N-values of the lacustrine sediments typically ranged from "weight of hammer" to 20 bpf, although some higher blow counts were observed, primarily at the contacts with underlying gravels. Typically, the blow counts were "weight of hammer" to 7 bpf, which indicates very loose sandy materials, and very soft to firm consistency in silts and clays. "Weight of hammer" refers to conditions where the sampler penetrated the soil under the weight of the hammer, without any hammer blows to drive the sampler.

### **3.2.3 SH 200 Bridge, Northwest Side**

Borings SH-C02, SW 4-1, and SW 4-2 were drilled in the vicinity of the northwest abutment of the SH 200 bridge. The lacustrine sediments at this location range in thickness from 2 feet in SW 4-2 to 12 feet in SW 4-1. SW 4-2 was drilled close to the bridge embankment and it appears that the upper several feet of the boring were advanced through bridge embankment materials. The sediments in SW 4-1 were described primarily as brown, very soft silt to very loose silty sand with minor clay and organic wood chips. N-values in the sediments in SW 4-2 ranged from 1 to 2 bpf. The top elevation of sediments in this area is at an elevation of approximately 3261 feet, and the bottom elevation of sediments (sediment/alluvium contact) is at approximately 3249 feet.

### **3.2.4 SH 200 Bridge, Southeast Side**

Borings SW 3-1 and SW 3-2 were drilled in the vicinity of the southeast abutment of the SH 200 bridge. The lacustrine sediments at this location range in thickness from approximately 12 to 13.5 feet. The sediments are described primarily as brown to gray, very soft lean clay and silt, to very loose, poorly graded sand. Blow counts in the sediments ranged from zero to five bpf. The top elevation of sediments in this area is at an elevation of approximately 3261 feet, and the bottom elevation of sediments (sediment/alluvium



contact) is at approximately 3240 feet. Note that because the two borings in this area were advanced from a barge, they did not penetrate the uppermost portion of the sediments.

### **3.2.5 I90 Bridges, Northwest Side**

Borings EM-C15, GC-C02, SW 1-1, SW 1-2, and SW 1-3, I-SW-1, and I-NW-2 were drilled in the vicinity of the northwest abutment and approach embankment of the I90 bridges. The lacustrine sediments in this vicinity range in thickness from 9 feet to 26.5 feet. The variability in sediment thickness is likely due to partial scouring by the Blackfoot River and possible removal or disturbance during embankment construction. The sediments are thickest in borings SW 1-1 and EM-C15, where no scour has occurred. The top elevation of sediment layer in this vicinity is approximately 3261.5 feet. The bottom elevation of the sediment layer at the sediment/alluvium contact in this vicinity ranges from approximately 3226 to 3240 feet.

The sediments in this vicinity include brown fine sand, silty sand, silt, and lean clay. Organic wood chips were also observed in the borings. As shown on the cross sections, the soil borings appear to indicate that a significant portion of the sediment layer is composed of sandy material, in layers that may be on the order of 5 feet thick or greater. This is consistent with observations of surface exposures along the shoreline south of the bridges.

It appears that the silt and clay soils are present in layers that are typically on the order of 2-feet to 4-feet thick. It is not clear if these layers are consistent from one boring to another, but they were generally encountered between approximate elevation 3239 feet and 3250 feet.

N-values in the sediments in this area ranged from one to 14 bpf.

### **3.2.6 I90 Bridges, Southeast Side**

Borings EM-C11, GC-C06, SW 2-1, SW 2-1B, SW 2-2, and SW 2-3 were drilled at the base of the southeast abutment of the I90 bridges. EM C-01 was drilled through the southeast abutment and penetrated the sediments. The lacustrine sediments in this vicinity range in thickness from 2 to 21 feet. The sediment thickness in this vicinity is variable due to partial scouring by the Blackfoot River, and the original relief of the alluvial deposits upon which the sediments were deposited. Also, borings SW 2-2 and SW 2-3 were drilled through embankment materials overlying the sediments. The top elevation of sediment layer in this vicinity is approximately 3261.5 feet. The elevation of sediment layer at the sediment/alluvium contact in this vicinity ranges from approximately 3227 to 3251 feet.

The sediments in this vicinity include soft gray lean clay to poorly graded, loose, fine sands. Very dark gray to black organic silty sands and sandy silts were also observed in this vicinity. Borings EM-C01 and EM-C11 indicate a 3-foot clay/silt layer between elevations 3257 to 3260. Below this material is several feet of sand and silty sand. Below that, much of the material from about elevation 3252 down to about 3240 is sandy silt to fat clay. Borings SW2-1, SW2-2, and SW2-3 indicate a very soft, gray clayey layer at approximately elevation 3248.

SPT N-values in the silts and clays in this area ranged from zero to three bpf, which indicated a very soft consistency in the silt and clay materials.



### 3.2.7 Alluvial Sands and Gravels

Alluvial sands and gravels underlie the reservoir sediments and overlie the argillite bedrock. The alluvium was deposited by the Clark Fork and Blackfoot Rivers and originally formed broad floodplains with multiple terrace levels near the confluence of the two rivers. The alluvium typically consists of poorly graded gravels with sands and silts, to silty gravels, with occasional sandy lenses. Based on soil boring information, this material is typically described as multi-colored, wet, sandy, coarse-grained, rounded sands and gravels composed of mixed lithologies. The pre-construction and sediment deposition surface of the alluvial deposits in the vicinity of the I90 bridges ranges from elevation 3227 to 3260. The surface of the alluvial deposits in the vicinity of the SH 200 bridge ranges from elevation 3226 to 3256.

The thickness of the alluvial sands and gravels in the project area ranges in thickness as a function of the configuration of the original bedrock surface upon which it was deposited. In the vicinity of the I90 bridges, the alluvium ranges from approximately 3 to 38 feet in thickness, based on soil boring information. In the vicinity of the SH 200 bridge, the argillite bedrock surface drops to the north, and consequently the alluvium is much thicker, and estimated to be between 80 and 100 feet thick.

Based on observations during the 2005 and 2006 drilling activities, and bulk core samples of the alluvium collected by Envirocon (EMC2, 2005), the particle sizes appear to range typically from sand-sized up to 6-inch cobbles, with occasional larger cobbles to boulders. The alluvial gravels are estimated to contain as much as 10 to 15 percent fines (particles passing #200 sieve). N-values of the alluvial materials ranged from 20 bpf to hammer refusal, which indicates medium-dense to very dense material.

### 3.2.8 Argillite Bedrock

Argillite bedrock underlies the alluvial deposits in the project area. Argillite is defined as weakly metamorphosed siltstone to claystone. Based on soil boring information, the argillite is typically described in lithologic terms as light greenish-gray to maroon, fine-grained, finely laminated, and thin-bedded. MDT had noted that zones of very hard argillite or quartzite are sometimes encountered, but none were found in the borings advanced by CH2M HILL. The average bedding dip appears to be approximately 20 degrees, based on measurements from core samples.

The argillite was encountered in several boreholes in the vicinity of the I90 bridges, where the depth of the argillite ranged from 14 to 77 feet below ground surface (the argillite was encountered at more shallow depths in the borings drilled in the vicinity of the river channel versus the borings drilled on top of the embankments). The elevation of the argillite surface near the I90 bridges ranges from approximately 3220 to 3232 feet. The surface of the argillite slopes down in elevation to the northeast; and therefore is deeper in the vicinity of the SH 200 bridge. Because of the greater depth to bedrock in the vicinity of the SH 200 bridge, argillite was only encountered in one of the borings, SH-C02, at an elevation of approximately 3194 feet.

The rock mass quality of the argillite varies throughout the project site. Much of the argillite is described as moderately to highly weathered, and moderately to intensely fractured (fracture spacing of >10 fractures/foot). The Rock Quality Designation (RQD) of the argillite



bedrock was predominantly in the "0 to 25 percent" range, which corresponds to "very poor rock mass quality" and is indicative of densely fractured rock. Twenty percent of the core runs showed RQD between 25 and 50 percent, which classified as "poor rock mass quality." Only 8 percent of the core runs showed RQD between 50 and 75 percent, which qualifies as "fair rock mass quality."

Fracture orientations ranged from vertical to horizontal, and fractures along 20-degree dipping bedding planes are common. Numerous distinctive highly weathered and fractured zones were observed within the argillite, where the core samples would break down to angular, granular fragments. The hardness of the argillite was estimated to be generally in the R2 to R3 range, based on field tests performed on the core samples. The R2 to R3 hardness corresponds with an estimated unconfined compressive strength between 800 and 7,000 psi. However, zones of estimated hardness of R1 (compressive strength less than 800 psi) were observed.

Based on the rock mass characteristics observed in the core samples of argillite; the argillite was generally divided into two types, labeled as Type 1 and Type 2 rock mass in this report. A description of the characteristics of each rock mass type follows.

### **3.2.9 Type 1 Rock Mass**

Type 1 rock mass is typically described as very weak, highly weathered, densely to intensely fractured argillite. The core samples of Type 1 argillite were noticeably weaker in strength and more weathered and fractured than Type 2 rock mass. Many of the Type 1 core specimens would crumble into granular material while handling the core, or easily break into small angular fragments during field testing. The RQD of Type 1 rock mass ranged from zero to 22 percent, with an average of less than 5 percent. The hardness of the Type 1 rock mass was typically estimated to be R1 to R3 (200 to 7,000 psi). No laboratory strength testing could be performed on core samples of Type 1 argillite due to the dense fracturing, which resulted in a lack of cores that met the length to width ratio required for compressive strength testing. The Rock Mass Rating (Bieniawski, 1989) for Type 1 ranges from 21 to 35, which indicates "Poor Rock Mass." Based on the rock mass characteristics and rock mass rating systems, the estimated Mohr-Coulomb parameters of the Type 1 rock are estimated to be a friction angle ( $\phi$ ) of 15 to 25 degrees, and a cohesion ( $c$ ) of 2,100 to 4,300 psi.

### **3.2.10 Type 2 Rock Mass**

Type 2 rock mass is typically described as slightly weathered and moderately fractured argillite. Based on field strength testing and laboratory testing, performed on the core specimens, the strength and durability of the Type 2 rock was higher than the Type 1 rock mass. The RQD of Type 1 rock mass ranged from less than 10 to 60 and averaged 22 percent. The hardness of the Type 1 rock mass was typically estimated to be R2 to R3 (800 to 7,000 psi). Laboratory testing confirmed the unconfined compressive strength of intact core specimens to be approximately 7,000 psi. The Rock Mass Rating (Bieniawski, 1989) for Type 2 ranges from 40 to 48, which indicates "Fair Rock Mass." Based on the rock mass characteristics and rock mass rating systems, the estimated Mohr-Coulomb parameters of the Type 2 rock are estimated to be a friction angle ( $\phi$ ) of 25 to 35 degrees, and a cohesion ( $c$ ) of 4,300 to 6,500 psi.



### 3.2.11 Distribution of Type 1 and Type 2 Argillite Bedrock

In order to evaluate the distribution of the two types of rock mass in the vicinity of the I90 bridge piers and abutments, the elevations and thickness of zones of Type 1 and Type 2 argillite bedrock were plotted based on elevations of borings drilled near the I90 bridge piers and abutments (argillite bedrock was not cored in the vicinity of SH 200). Borings I90PB-1, I90BP-2, EB-2, SW1-1, SW1-2, SW2-1, and SW2-2 were drilled and logged by CH2M HILL personnel in March and April 2006, and therefore the core samples of the bedrock were available for visual examination, field testing, and laboratory testing. Borings GC-C01, GC-C02, GC-C06, GC-C07, and GC-C09 were logged by Envirocon personnel; so the actual core samples were not available for visual examination or testing. Therefore, the determination of which of the cores from these borings classifies as Type 1 versus Type 2 categories from these drill holes is based solely on boring logs provided by Envirocon.

The elevation and thickness of Type 1 and Type 2 rock are summarized in Table 3-1. As shown in Table 3-1, the estimated thickness of Type 1 rock ranges from zero up to 17 feet in thickness. The elevations at which Type 1 rock transitions into Type 2 rock ranges from approximately 3205 to 3226 feet. It is evident that the thickness and elevations of rock mass types vary across the project site. The thickness of Type 1 and Type 2 rock is discussed later for specific areas of the project.

Several basic assumptions were made when estimating the thickness of Type 1 rock mass, and the elevations where the Type 1 rock mass transitions to Type 2 rock mass. First, the upper portion of the argillite in general appears to be more weathered and fractured, which is typical in a subsurface bedrock profile due to weathering near the rock surface. Therefore, zones of Type 1 rock are typically found near the upper surface of the bedrock, and the bedrock transitions at some point at depth into Type 2. However, zones of highly fractured and weathered argillite were observed within the Type 2 rock mass. The orientations and extent of these fracture zones are not known; they may "daylight" in other areas at a distance away from the boring.

In addition, the thickness of the Type 1 rock mass and the elevations where the Type 1 rock transitions to Type 2 at each boring are only valid at that boring location. Based on rock core data, the argillite is highly variable in rock mass properties, such as the degree of weathering and density of fracturing. It is therefore likely that the thickness of Type 1 rock mass, and the elevations at which Type 1 rock mass transitions into Type 2 rock mass are variable in the vicinity of the I90 bridges. For example, the estimated thickness of Type 1 rock mass at I90BP-1 is 15 feet; whereas the estimated thicknesses of Type 1 rock at borings SW1-1 and SW2-1, on either side of I90BP-1, are zero and 5 feet, respectively. This example illustrates the variability of the rock mass properties and suggests that caution be used when estimating the rock mass properties of the argillite bedrock.



**TABLE 3-1**  
Estimated Limits of Bedrock Type 1 and Type 2 Elevations

| Boring with Cores                            | EB-2   | SW1-1  | SW1-2  | SW2-1  | SW2-2  | I90BP-1 | I90BP-2 | GC-C01 | GC-C02 | GC-C06 | GC-C07 | GC-C09 |
|--|--------|--------|--------|--------|--------|---------|---------|--------|--------|--------|--------|--------|
| Top of Bedrock Elevation (ft)                | 3227.2 | 3220.1 | 3225.0 | 3231.6 | 3227.4 | 3227.2  | 3224.3  | 3223.8 | 3222.4 | 3220.5 | 3223.3 | 3224.4 |
| Top of Type 1 Rock Elevation (ft)            | 3227.2 | na     | 3225.0 | 3231.6 | 3227.4 | 3227.2  | 3224.3  | 3223.8 | 3222.4 | 3220.5 | 3223.3 | na     |
| Estimated Elevation, top of Type 2 Rock (ft) | 3219.2 | 3220.1 | 3224.0 | 3226.6 | 3222.4 | 3212.2  | 3213.3  | 3211.8 | 3205.4 | 3205.5 | 3213.3 | 3224.4 |
| Estimated Thickness of Type 1 Rock (ft)      | ≥8     | 0.0    | 1.0    | 5.0    | 5.0    | 15.0    | 11.0    | 12.0   | 17.0   | 15.0   | 10.0   | 0.0    |
| Total Depth (ft)                             | 42.0   | 50.0   | 42.0   | 34.0   | 50.5   | 50.0    | 50.0    | 35.5   | 43.0   | 49.0   | 72.5   | 65.0   |
| Bottom of Boring Elevation (ft)              | 3219.2 | 3211.5 | 3213.5 | 3218.4 | 3205.0 | 3188.2  | 3188.6  | 3202.8 | 3200.4 | 3200.5 | 3166.8 | 3173.4 |

Notes:

na = no Type 1 rock; only Type 2 rock observed  
Elevations are NAVD 88.1



### 3.3 Groundwater Conditions

The groundwater elevation in the project vicinity is closely related to the elevation of Milltown Reservoir and the resulting saturation of the sediments due to recharge from the reservoir water. The depth to groundwater in the sediment flats ranges from 0.5 to 2.7 feet below ground surface (elevation ranges between 3260.3 and 3261.8), based on measurements from borings drilled at the foot of the embankments. The depth to groundwater in the borings drilled through the bridge and highway embankments ranges between 23 and 43.8 feet below ground surface. However, the groundwater elevations based on these borings may be inaccurate, because fluids were pumped into the borings during the drilling, and the depth-to-water readings taken in these borings may have been recorded prior to the water levels stabilizing. Table 3-2 provides a summary of depth to groundwater and groundwater elevations.

**TABLE 3-2**  
Summary of Groundwater Elevations

| Boring | Elevation<br>(ft amsl) | Depth to Water*<br>(ft) | Groundwater Elevation<br>(ft amsl) |
|--------|------------------------|-------------------------|------------------------------------|
| EM-C01 | 3290.60                | 30                      | 3260.6                             |
| EM-C02 | 3279.50                | 31                      | 3248.5                             |
| EM-C03 | 3280.90                | 20.3                    | 3260.6                             |
| EM-C04 | 3285.00                | 24                      | 3261.0                             |
| EM-C05 | 3292.40                | 34                      | 3258.4                             |
| EM-C06 | 3261.40                | 0.5                     | 3260.9                             |
| EM-C07 | 3262.60                | 1                       | 3261.6                             |
| EM-C08 | 3262.60                | 2.7                     | 3259.9                             |
| EM-C09 | 3261.80                | 1.6                     | 3260.2                             |
| EM-C10 | 3261.60                | 1.7                     | 3259.9                             |
| EM-C11 | 3261.50                | 1.6                     | 3259.9                             |
| EM-C12 | 3282.60                | 23                      | 3259.6                             |
| EM-C14 | 3290.20                | 43.8                    | 3246.4                             |
| EM-C15 | 3299.70                | 38.7                    | 3261.0                             |
| EM-C17 | 3310.60                | 40                      | 3270.6                             |
| EM-C21 | 3302.80                | 38                      | 3264.8                             |
| SH-C01 | 3291.00                | 34                      | 3257.0                             |
| SH-C02 | 3287.30                | 43.5                    | 3243.8                             |

Notes:

\* Depth to groundwater based on measurements from field logs.  
Elevations are NAVD 88.



## **3.4 Predicted Scour and Blackfoot River Water Surfaces**

Predicted scour was discussed in the Draft Milltown Bridge Infrastructure Mitigation Report (CH2M HILL, 2005). A final hydraulics report was prepared in order to provide scour estimates to be used in mitigation design (Milltown Bridge Infrastructure Mitigation Hydraulics Report, CH2M HILL, 2006a). The following is a summary of the results of the scour analysis. The hydraulics report contains detailed methodology and calculations of scour estimates.

### **3.4.1 Scour Conditions**

The scour conditions that affect the project include general scour, contraction scour, and local scour. These are expected to affect the piers of the structure and the abutments. In addition to the scour, there is a potential for movement of the channel thalweg. Scour conditions at the piers and abutments are discussed below.

#### **3.4.1.1 Interstate 90 Bridge Piers**

Following removal of the dam, the center piers of both interstate bridges will be susceptible to increased local scour during flood events. These piers are founded on weathered argillite bedrock.

Hydraulic Engineering Circular 18 (HEC-18) Evaluating Scour at Bridges (FHWA, 2001) provides guidelines for evaluating existing bridges for vulnerability to scour and improving the state-of-practice of estimating scour at bridges. HEC-18 is widely accepted and used to estimate scour at bridges. However, the methods and equations provided in HEC-18 are for determining scour depths in non-cohesive soils and are therefore not considered applicable for analysis of the weathered argillite at the I90 bridges.

In order to evaluate scour at the interstate bridges, it is imperative to determine if the weathered argillite is resistant to scour. HEC-18 includes 10 pages in an appendix that discuss scour competence of rock formations and concludes that "additional research is needed in this area." HEC-18 briefly describes the Erodibility Index Method developed by George Annandale to quantify the relative ability of non-uniform earth material to resist erosion. Annandale's Erodibility Index Method was used to estimate the potential depth of scour into the weathered bedrock. Details of how the method was applied can be found in the Milltown Bridge Infrastructure Mitigation Hydraulics Report (CH2M HILL, 2006a). Results of the scour estimates are included in Table 3-3. The erodibility index method indicates that the local scour will occur within the weathered argillite, to the contact with Type II Argillite, as described earlier; at approximate elevation 3212 feet.

#### **3.4.1.2 SH 200 Bridge Piers**

Following removal of the dam, the center pier at the SH 200 Bridge will also be susceptible to increased local scour during flood events. HEC-18 provides guidelines for evaluating existing bridges for vulnerability to scour and improving the state-of-practice of estimating scour at bridges. HEC-18 is widely accepted and used to estimate scour at bridges. To determine local pier scour, an equation based on the CSU equation is recommended for both live-bed and clear-water pier scour. Table 3-3 summarizes results of the scour calculations at the SH 200 Bridge.



### 3.4.1.3 General Scour at Abutments

The concept design included estimates of scour of approximately 6.8 feet, and 2.4 feet, occurring at the I90 structures, and SH 200 structures, respectively, for the 475-year flood.

This scour was considered in the slope stability analysis by assuming that the soil was eroded to the total depth of scour along the entire wetted perimeter, and that the abutment slopes would erode as necessary to establish a maximum slope of 1.5H:1V.

Based on this analysis, it was considered that mitigation measures were necessary to maintain stability of the abutments. However, introduction of a temporary stabilization wall creates the potential for local scour, if the channel thalweg moves to the face of the wall.

### 3.4.1.4 Thalweg Movement

The combination of thalweg migration to a stabilization wall and local scour at the toe of the wall predicts the possibility of vertical walls from 40-feet to 48-feet high. CH2M HILL structural and geotechnical engineers have evaluated numerous alternatives for design of this type of stabilization wall and concluded that walls of this height are not practical, considering the cost and length of time that would be required for construction. Because the face of the wall would not be accessible during construction (before scour), it would not be possible to install anchors to resist lateral earth forces. Therefore, cantilever walls would be required to address this extreme occurrence. A 40-feet-high cantilever wall is not feasible as well, so other alternatives were investigated.

Based on the considerations above, CH2M HILL recommended that jet grouting methods be used to stabilize the slope. Jet grouting refers to a process by which high-pressure fluids or binders are injected into the soils at high velocities to create a soil-cement or soilcrete mass. The grouting is accomplished by drilling to the required treatment depth, and then injecting grout as the tools are rotated and retracted. The binders erode and break up the soil structure, and mix with the soil particles in situ to create a homogeneous mass. After curing, the soilcrete has much higher shear strength than the untreated soil.

The jet grout mass will be designed to maintain stability of the slope during the drawdown, and during scour events, if the thalweg moves closer to the bridge foundations. Details of this stability analysis are presented in Section 4.0 Slope Stability Evaluation.

For local scour at the I90 bridge piers, it was assumed, based on erodibility index calculations, that the scour will not occur below the estimated top elevation of the Type 2 argillite. No evaluation of bedrock scour was conducted at the SH 200 bridge; as bedrock is estimated to be at approximately elevation 3150 feet at this location. The extent of local contraction and pier scour were estimated for each of the three bridges. Table 3-3 shows a summary of local scour at the bridge center piers.



**TABLE 3-3**  
Summary of 500-Year Pier Scour Calculations

| Bridge        | Method                               | Scour Depth (ft) | Scour Elevation (ft) | Existing Bottom of Footing Elevation (ft) | Proposed Bottom of Drilled Shaft Elevation (ft) |
|---------------|--------------------------------------|------------------|----------------------|---|---|
| I90 Eastbound | Erodibility Index Method             | 18.64            | 3212 <sup>1</sup>    | 3236.98                                   | See note  |
| I90 Westbound | Erodibility Index Method             | 19.84            | 3212 <sup>1</sup>    | 3233.00                                   | See note  |
| SH 200        | HEC-18 CSU Equation for Complex Pier | 14.51            | 3223.62              | 3228.59                                   | to be designed <sup>2</sup>                     |

Notes:

<sup>1</sup> Estimated elevation of interface between Type 1 and Type 2 argillite bedrock

<sup>2</sup> Design of pier underpinning has not been completed as of completion of this report.

### 3.4.2 Blackfoot River Water Surface Elevations

Table 3-4 summarizes the water surface elevations at each bridge that are used as input for the evaluation of foundations and stability of the Blackfoot River bridges. The water surfaces at each stage of reservoir drawdown are shown, as well as post-drawdown elevations for the ordinary high-water (1.5-year) flow, average flow, 100-year flood event, and 500-year flood event.

**TABLE 3-4**  
Predicted Water Surface Elevations

|   | SH 200  | I90 Westbound | I90 Eastbound |
|---|---------|---------------|---------------|
| Pre-Dam Removal Normal Operating Full Pool Elevation (ft)                   | 3261.8  | 3261.8        | 3261.8        |
| Predicted End of Stage 1 Drawdown Water Surface Elevation (ft) <sup>1</sup> | 3254.0  | 3254.0        | 3254.0        |
| Predicted End of Stage 2 Drawdown Water Surface Elevation (ft)              | 3249.5  | 3249.5        | 3249.5        |
| Ordinary High Water Surface Elevation (ft) <sup>3</sup>                     | 3248.44 | 3246.78       | 3245.08       |
| Average Water Surface Elevation (ft) <sup>4</sup>                           | 3242.11 | 3240.08       | 3239.68       |
| Predicted 100-year Flood Water Surface Elevation (ft)                       | 3259.27 | 3257.82       | 3256.89       |
| Predicted 500-year Flood Water Surface Elevation (ft)                       | 3260.78 | 3259.13       | 3258.05       |

Notes:

1. Water surfaces were taken from Figure 5 of the Draft Scour Evaluation, Addendum 2, August 2, 2005.

2. See Figure 5 of the Final RD/RA Statement of Work for a timeline of the stage drawdowns.

3. Ordinary High Water Surface ( $Q_{1.5}$ ) was evaluated by additional modeling summarized in the Hydraulics Report (CH2M HILL, 2006c). These water surface elevations approximately correspond to a Blackfoot River flow of 7,120 cfs.

4. Average Water Surface ( $Q_{AVG}$ ) was evaluated by additional modeling summarized in the Hydraulics Report (CH2M HILL, 2006c), where the 1999 flows were taken to be representative of the long-term average water surface at the end of Stage 3 drawdown, following reservoir drawdown and dam removal. These water surface elevations approximately correspond to a Blackfoot River flow of 1,645 cfs.



### 3.5 Seismicity

The maximum considered earthquake (MCE) event corresponds to an event having a 2 percent probability of exceedance in 50 years (or 2,475-year return period). For the Milltown site, the MCE has a peak ground acceleration (PGA) of approximately 0.25g at the bedrock surface. This value of PGA on rock is an average representation of the acceleration most likely to occur at the site for all seismic events (crustal, intraplate, or subduction). The corresponding PGA for an event having a 10 percent probability of exceedance in 50 years (or 475-year return period) is approximately 0.11g.

Seismic deaggregation mapping was used for selection of the most probable earthquake magnitude for the Milltown site. This resource provides an estimate of earthquake magnitude at discrete locations, considering the percent contribution of all potential sources for an area (subduction, intraslab, and crustal), as developed by the United States Geological Survey (USGS) Seismic Hazard Mapping Project. Based on input of latitude and longitude for the project site, the highest statistical contribution is for a seismic event with a magnitude of approximately 6.7, for a 2,475-year mean return period (USGS, 2003); for an event having a 475-year mean return period, the approximate magnitude is 6.4.

#### 3.5.1 Seismic Parameters

Seismic design parameters were developed in accordance with the International Conference of Building Officials and USGS *Seismic Design Parameters, Version 3.10* (ICBO, 2003). The site should be designed according to Site Class C. Parameters for Site Class B are also presented. The corresponding seismic design parameters are summarized in Table 3-5.

**TABLE 3-5**  
Seismic Design Parameters

| Site Class                                     | Earthquake Magnitude | Peak Horizontal Ground Acceleration on Bedrock | Soil Amplification Factor, $F_a$ | Peak Horizontal Ground Acceleration at Ground Surface |
|--|----------------------|--|----------------------------------|---|
| 2% Probability of Exceedence in 50 Years (MCE) |                      |  |                                  |   |
| S <sub>B</sub>                                 | 6.7                  | 0.25g  | 1.00                             | 0.25g   |
| S <sub>C</sub>                                 | 6.7                  | 0.25g  | 1.15                             | 0.28g   |
| 10% Probability of Exceedence in 50 Years      |                      |  |                                  |   |
| S <sub>B</sub>                                 | 6.4                  | 0.11g  | 1.00                             | 0.11g   |
| S <sub>C</sub>                                 | 6.4                  | 0.11g  | 1.20                             | 0.14g   |

g = The acceleration due to gravity.

The following additional parameters for the MCE are presented for structural design:

- Short period (0.2s) spectral response acceleration,  $S_{MS} = 0.62g$  for Site Class S<sub>B</sub>;  $S_{MS} = 0.71g$  for Site Class S<sub>C</sub>.
- 1-second period spectral response acceleration,  $S_{M1} = 0.19g$  for Site Class S<sub>B</sub>;  $S_{MS} = 0.31g$  for Site Class S<sub>C</sub>.



For the event having a 10 percent probability of exceedance in 50 years (475-year return event), the spectral accelerations are as follows:

- Short period (0.2s) spectral response acceleration,  $S_{MS} = 0.28g$  for Site Class  $S_B$ ;  $S_{MS} = 0.34g$  for Site Class  $S_C$ .
- 1-second period spectral response acceleration,  $S_{M1} = 0.08g$  for Site Class  $S_B$ ;  $S_{MS} = 0.14g$  for Site Class  $S_C$ .

### 3.5.2 Liquefaction Potential

Liquefaction is a temporary loss of shear strength in soil that can occur during seismic events of sufficient magnitude to cause a significant increase in pore pressure. Liquefaction generally occurs in clean sandy or silty soils that are saturated and have a loose or very loose consistency. Within the lacustrine sediment layer, observations in the field and review of boring logs indicate a high frequency of sandy interbeds. Some of these sandy layers within the sediments are estimated to be up to 5 feet thick.

A detailed evaluation of liquefaction potential was not performed. However, a preliminary evaluation of liquefaction was conducted to evaluate the general potential within the lacustrine sediment layer. This evaluation was performed for both the MCE, and for the 475-year return period event (10 percent probability of exceedance in 50 years). Other details of seismic parameters at the Milltown site are presented in Section 3.5.1. This evaluation considered the ordinary high water (Q1.5) presented in Table 3-4.

Two evaluations of liquefaction potential were performed. The first evaluation was performed as part of the Draft Milltown Bridge Infrastructure Mitigation report (CH2M HILL, 2005). In this evaluation, 22 borings advanced by others were analyzed for liquefaction potential. For the 475-year return period event, the liquefaction potential was found to be insignificant. For the MCE, it appears that an average thickness of 1 to 2 feet of the sediments may liquefy, or a maximum thickness of 10 feet in localized areas.

In a more general analysis, all of the SPT N-values within the lacustrine sediment were organized in a histogram plot, and the ranges of values with the highest statistical contribution were evaluated. This evaluation suggests that for the 475-year return period event, silty sands with an uncorrected N-value of 2 or less would have a low liquefaction potential (factor of safety near 1.0). For clean sands and gravels, material with an N-value of 4 or less would be susceptible to liquefaction. Layers with these properties account for approximately 10 percent of the data collected within the lacustrine sediments layer. For the MCE, silty sands with an N-value of 6 or less, and clean sand and gravel layers with an N-value of 8 or less would be susceptible to liquefaction. Layers with these properties account for approximately 25 percent of the data collected from the lacustrine sediments layer. To sum this second evaluation up very roughly, it could be assumed that approximately 10 percent of the lacustrine sediments layer may liquefy during the 475-year return period of the sediments are saturated. This percentage goes up to 25 percent for the MCE.

Because of the presence of these sandy interbeds within the lacustrine sediments, there may be areas at the project site that are susceptible to liquefy during a long-duration or high-magnitude event.

Additional liquefaction analyses were completed using the more recent data. Within the lacustrine sediments, Shelby tubes and oversized 3-inch O.D. split spoon samplers were frequently used to maximize the amount of soil recovered for soil testing. N-values associated with a 3-inch oversized sampler are not equivalent to a standard 2-inch O.D. sampler. A limited liquefaction assessment was performed using SPT N-values from sand and silty sand layers from borings. Below the I90 northwest abutments and approach embankment, sand interbeds identified in Boring SW1-1 (from elevation 3244 to 3248 feet) have a factor of safety against liquefaction,  $FS_{liq}$ , of 1.0 for a 475-year seismic event. This indicates the potential for the loose, saturated sand interbeds below the northwest abutments to liquefy. The boring log for GC-C02 indicates loose saturated sands from elevation 3233 to 3238 feet that may liquefy. Loose sand layers identified in Borings EB-2 (near the toe of the I90 embankment, west of Blackfoot River from elevation 3249 to 3252 feet) and EM-C11 (near the toe of the I90 embankment, east of the Blackfoot River from elevation 3251 to 3254) have a  $FS_{liq}$  of less than 1.0, but are located above the ordinary high water level.

Greater or lesser amounts of liquefaction could occur for seismic events of different magnitude and duration. The final design of the slope stabilization measures will have to include consideration of liquefaction in the seismic stability analysis. This is typically based on estimates of residual strengths for the liquefied material that are based on correlations with SPT N-values.



## 4.0 Slope Stability Evaluation

---

The stability of approach embankments for the I90 and SH 200 Bridges has been a chief concern associated with the remediation of the Milltown site. The following section discusses the estimated properties for the materials influencing stability, the stability of the slopes under the existing conditions, and the effects of the mitigation measures.

Note that much of the stability analysis was previously performed prior to preparation of the Jet Grout Stabilization Design Package. During initial jet grout operations in October 2006, a slope failure occurred. This failure will be discussed in separate documents to be prepared after consultation with MDT geotechnical engineers. However, it is referenced here, where it is relevant to the shear strength evaluation.

### 4.1 Soil Properties for Stability Analysis

Discussions of the relevant soil properties are provided separately for each of the major units identified in the Subsurface Conditions section of this report.

#### 4.1.1 Embankment Fill

The existing fill material used to construct the I90 embankments appears to consist of sandy gravel. Based on the laboratory testing presented in the Envirocon Data Summary Report #3 (Envirocon, 2005a) the fill appears to typically consist of about 70 percent gravel-sized particles, and is typically classified as poorly graded gravel.

Because of the presence of the gravel and cobbles, and because the material is not cohesive it is difficult to obtain samples for shear strength testing. The original stability analyses used an assumed angle of internal friction equal to 35 degrees, and a total unit weight of 120 pcf for the gravel material. During review of stability analyses, MDT requested that higher unit weights be considered. It is possible that higher unit weights exist for the fill because it was likely compacted, although not necessarily to the standards that would be required today. Therefore, subsequent stability analysis used a unit weight of 135 pcf, with an angle of internal friction of 38 degrees.

The stability analyses have generally indicated that the results are not very sensitive to the variations in properties used for the fill material, as long as the values correspond (that is, the appropriate range of unit weight is used in conjunction with the appropriate strength). Because it may be necessary to complete additional stability analyses to revise the slope stabilization design, a more detailed evaluation of the SPT N-values was made, so that they could be used to estimate the angle of internal friction for the material. SPT N-values appear to indicate that the material is typically medium-dense, and the classifications indicate that it is typically poorly graded gravelly material. Based on charts by Naval Facilities Engineering Command (NAVFAC, 1982) it appears that a dry unit weight ranging from about 118 to about 125 pcf is the appropriate range (Figure 9). Moisture contents from laboratory testing indicated moisture contents typically less than 5 percent, but assuming moisture content of 7 percent, to be conservative, the moist unit weight is estimated to be



127 to 134 degrees. The corresponding range for the angle of internal friction is 33 degrees to 38 degrees. Therefore, it is recommended that future stability analyses be completed using an estimated total unit weight of 130 pcf, and an angle of internal friction of 35 degrees.

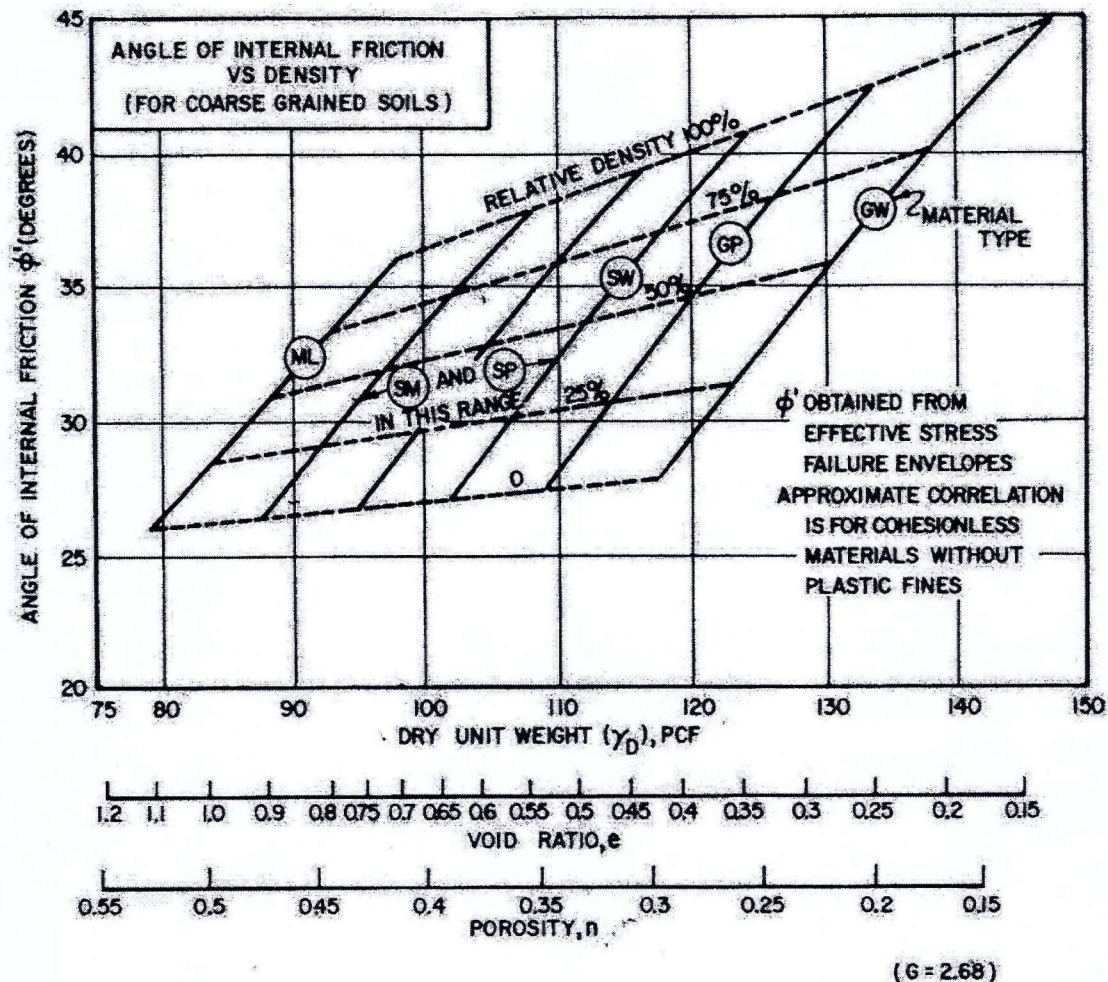


FIGURE 9  
Angle of Internal Friction Versus Relative Density (NAVFAC, 1982).

#### 4.1.2 Sediment

The sediment consists of interlayered clay, silt, and sand, and mixtures of these particle sizes.

In the stability analyses completed to date, the sediment unit has been treated as a layer of clay, with strength properties evaluated from the findings of triaxial testing. This was considered a conservative assumption because the failure surfaces that influence the design are relatively deep, and use of drained envelopes in sandier material would result in greater shear strength.



However, in order to avoid excessive conservatism, the distribution of material within the sediment layer has been considered in greater detail. It appears that the sediment typically includes sandier material in the upper several feet, with clay layers in the lower portion of the unit.

#### 4.1.2.1 Sandy Sediment

N-values in the sand sediment materials range from 0 to 22 bpf. It is assumed that the material is typically very loose to loose. Based on this N-value, and NAVFAC design charts, a dry unit weight of about 93 pcf, and an angle of internal friction of 28 degrees would be estimated.

Direct shear tests were performed on four samples of sediment material that were either silty sand or dual classification (SP-SM) material. The results of these tests are summarized in Table 4-1. In summary, these tests resulted in friction angles of 35 to 40 degrees for the peak strength, and 32 to 34 degrees for the ultimate condition. The cohesion intercept from the direct shear testing has been ignored.

**TABLE 4-1**  
Index Properties and Direct Shear Results

| Boring ID | Sample ID | Sample Depth (feet) | Soil Class (ASTM D2487) | P200 (%) | LL (%) | PI (%) | Direct Shear Test Results |              |                       |              |
|-----------|-----------|---------------------|-------------------------|----------|--------|--------|---------------------------|--------------|-----------------------|--------------|
|           |           |                     |                         |          |        |        | Peak Shear Stress         |              | Ultimate Shear Stress |              |
|           |           |                     |                         |          |        |        | c (psf)                   | $\phi$ (deg) | c (psf)               | $\phi$ (deg) |
| EM-C08    | --        | 4.5 to 5.0          | MH                      | 99.8     | 52     | 21     | 150.5                     | 33.4         | 114.5                 | 32.0         |
| EM-C08    | --        | 15.0 to 17.0        | SM                      | 36.6     | NP     | NP     | 66.5                      | 34.7         | 79.0                  | 33.4         |
| EM-C09    | ST #4     | 5.0 to 7.0          | SP-SM                   | 8.0      | NP     | NP     | 209.6                     | 37.5         | 20.6                  | 34.3         |
| EM-C09    | BC #8B    | 12.5 to 13.0        | ML                      | 94.4     | 45     | 14     | 86.4                      | 34.2         | 89.5                  | 33.4         |
| EM-C09    | ST #10    | 15.0 to 17.0        | ML                      | 75.4     | 41     | 12     | 115                       | 32.0         | 103                   | 31.9         |
| EM-C10    | A         | 5.0 to 7.0          | SM                      | 30.8     | NP     | NP     | 60                        | 39.6         | 84.5                  | 31.8         |
| EM-C11    | BC #85    | 12.5 to 13.0        | CH                      | 98.3     | 62     | 31     | 0                         | 32.9         | 0                     | 33.2         |
| EM-C11    | E         | 15.0 to 17.0        | ML                      | 63.9     | NP     | NP     | 60                        | 33.8         | 66                    | 33.4         |
| EM-C17    | --        | 42.0 to 42.5        | SC-SM                   | 45.7     | 23     | 5      | 350                       | 30.3         | 332                   | 30.4         |
| SH-C01    | --        | 51.5 to 53.0        | SM                      | 22.3     | NP     | NP     | 78                        | 35.6         | 0                     | 34.6         |

**Notes:**

P200 = Percent passing the No. 200 sieve

LL = Liquid Limit

PI = Plasticity Index

NP = non-plastic

c = cohesion

$\phi$  = friction angle

Three triaxial shear tests were performed on samples of sediment material that consisted of sand to silty sand. The findings from these tests are included in Table 4-2, and indicated angles of internal friction of 29, 33, and 40 degrees. These friction angles are based on

subjective review of the stress paths to estimate the failure stress, as described in detail for the silty and clayey sediment samples. This was done because using the standard approach of determining failure by either the maximum principal stress ratio, or the maximum shear stress, would have resulted in very high friction angles that are not typical of these materials. Although it is not believed that there is a mistake in the laboratory testing (the results are consistent with the direct shear testing and are consistent between two different labs), it is not clear the actual mechanism that triggers these high strengths and as a matter of conservatism they are not used in the analysis.

Based on these various results, it is the opinion of CH2M HILL that the appropriate angle of internal friction angle for the sandy material in the stability analysis is on the order of 32 degrees. Previous stability analyses used a value of 31 degrees for all of the sediment, so this is believed to be acceptable.

MDT has expressed concern about the ultimate or residual strengths, occurring at very high strains. Discussions of residual strength behavior are provided by Stark and Eid (1997) and Mitchell (1993) discusses residual strength behavior, and indicates that for soil with low clay fraction there is no reduction in strength beyond the critical state strength. Since the results of triaxial testing on sandy materials indicated very high gains in strengths with continued shearing, and a relatively low value is already used, it is recommended no reduction in strength for large strain conditions be used for the sandy material within the sediment unit.

#### 4.1.2.2 Silt and Clay Sediments

Many triaxial shear tests have been performed on material from the sediment unit, focusing on the silt and clay layers in particular. A summary of the triaxial testing is presented in Table 4-2.

**TABLE 4-2**  
Shear Strength Data from Isotropically Consolidated, Undrained, Triaxial Shear Tests

| Boring and<br>Sample ID | %<br>fines | LL | PI | Classification | Initial Eff.<br>Confining<br>Stress, $\sigma'_0$<br>(psf) | Failure Data                         |                                      | Envelope   |                 |
|-------------------------|------------|----|----|----------------|---|--------------------------------------|--------------------------------------|------------|-----------------|
|                         |            |    |    |                |   | $(\sigma'_1 + \sigma'_3)/2$<br>(psf) | $(\sigma'_1 - \sigma'_3)/2$<br>(psf) | c<br>(psf) | $\phi$<br>(Deg) |
| EB2 ST2                 | 91         | 56 | 22 | MH             | 1440  | 1261                                 | 771                                  |            |                 |
| EB2 ST8                 | 85         | 48 | 20 | ML             | 806.4   | 1317                                 | 813                                  |            |                 |
| EB2 ST9                 | 62.0       | 23 | NP | ML             | 676.8   | 680                                  | 248                                  |            |                 |
|                         |            |    |    |                | 1296  | 1328                                 | 680                                  |            |                 |
| SW 1-3 5ST              | 97         | 70 | 37 | CH             | 2160  | 1919                                 | 1122                                 | 20         | 36              |
|                         |            |    |    |                | 1440  | 1764                                 | 1053                                 |            |                 |
|                         |            |    |    |                | 619.2   | 1336                                 | 789                                  |            |                 |
| SW 2-1B 3ST             | 93         | 52 | 22 | MH             | 2016  | 1619                                 | 899                                  |            |                 |
| CD C03<br>5.5 to 7.0    | 95         | NP | NP | ML             | 1440  | 1220                                 | 653                                  | 0          | 35              |
|                         |            |    |    |                | 2880  | 2392                                 | 1254                                 |            |                 |
|                         |            |    |    |                | 5760  | 3757                                 | 2087                                 |            |                 |



**TABLE 4-2**  
Shear Strength Data from Isotropically Consolidated, Undrained, Triaxial Shear Tests

| Boring and<br>Sample ID | %<br>fines | LL   | PI   | Classification | Initial Eff.<br>Confining<br>Stress, $\sigma_0'$<br>(psf) | Failure Data                         |                                      | Envelope   |                 |
|-------------------------|------------|------|------|----------------|---|--------------------------------------|--------------------------------------|------------|-----------------|
|                         |            |      |      |                |   | $(\sigma_1' + \sigma_3')/2$<br>(psf) | $(\sigma_1' - \sigma_3')/2$<br>(psf) | c<br>(psf) | $\phi$<br>(Deg) |
| EMC 6<br>16.5 to 18.5   | 84.8       | 49.1 | 23.5 | CL             | 1500  | 1157                                 | 702                                  | 51         | 34              |
|                         |            |      |      |                | 3000  | 1796                                 | 1024                                 |            |                 |
|                         |            |      |      |                | 6000  | 4321                                 | 2454                                 |            |                 |
| EMC 3<br>38 to 40       | 58.4       | 34.7 | 6.2  | ML             | 1500  | 1315                                 | 803                                  | 26         | 36              |
|                         |            |      |      |                | 3000  | 2337                                 | 1396                                 |            |                 |
|                         |            |      |      |                | 6000  | 4356                                 | 2600                                 |            |                 |
| EMC 7<br>7.0 to 9.0     | 6.3        | NP   | NP   | SP             | 1500  | 2109                                 | 1214                                 | 130        | 29              |
|                         |            |      |      |                | 3000  | 3518                                 | 1699                                 |            |                 |
|                         |            |      |      |                | 6000  | 6985                                 | 3521                                 |            |                 |
| EMC 7<br>12 to 14       | 73.8       | 40   | 12.5 | ML             | 1500  | 1277                                 | 900                                  | 316        | 31              |
|                         |            |      |      |                | 3000  | 2313                                 | 1502                                 |            |                 |
|                         |            |      |      |                | 6000  | 4220                                 | 2425                                 |            |                 |
| EMC 8<br>11.5 to 13.5   | 97.4       | 58.9 | 28   | MH             | 1500  | 1412                                 | 934                                  | 220        | 34              |
|                         |            |      |      |                | 3000  | 2086                                 | 1382                                 |            |                 |
|                         |            |      |      |                | 6000  | 3948                                 | 2360                                 |            |                 |
| EMC 9<br>10 to 12       | 73.5       | 39.6 | 13   | ML             | 500   | 464                                  | 343                                  | 10         | 42              |
|                         |            |      |      |                | 1250  | 1164                                 | 732                                  |            |                 |
|                         |            |      |      |                | 2500  | 1854                                 | 1273                                 |            |                 |
| EMC 11<br>10 to 12      | 94.6       | 49.6 | 23   | CL             | 500   | 499                                  | 322                                  | 7          | 38              |
|                         |            |      |      |                | 1250  | 921                                  | 550                                  |            |                 |
|                         |            |      |      |                | 2500  | 2077                                 | 1276                                 |            |                 |
| EMC 15<br>44 to 46      | 43.3       | NP   | NP   | SM             | 1000  | 914                                  | 432                                  | 0          | 40              |
|                         |            |      |      |                | 2000  | 1921                                 | 1116                                 |            |                 |
|                         |            |      |      |                | 4000  | 3821                                 | 2312                                 |            |                 |
| GC C02<br>10.5 to 11    | 2.5        | NP   | NP   | SP             | 1440  | 1761                                 | 983                                  | 0          | 33              |
|                         |            |      |      |                | 2880  | 3230                                 | 1588                                 |            |                 |
|                         |            |      |      |                | 5760  | 4743                                 | 2597                                 |            |                 |
| SW C01<br>11.1 to 12.5  | 95         | 59   | 24   | MH             | 1440  | 1112                                 | 652                                  | 0          | 35              |
|                         |            |      |      |                | 2880  | 2035                                 | 912                                  |            |                 |
|                         |            |      |      |                | 5760  | 3985                                 | 2257                                 |            |                 |

Standard practice for interpretation of strength from triaxial shear tests (Holtz and Kovacs, 1981) is to determine the stresses at failure based on either the maximum shear stress that occurs during the test, or based on the maximum principal stress ratio. Using these criteria resulted in relative high shear strengths (high undrained shear strengths and high angles of internal friction) because of the strain hardening behavior. The axial strain at failure according to these criteria was typically very high (e.g., 15 percent).

As an alternative, we considered using the shear stress corresponding to a specific value of strain (e.g., the shear strength corresponding to 2 percent strain for each specimen) to determine "failure" of the specimen. However, there is no basis in precedence or guidance from standard soil mechanics texts for selecting a value of strain for this method. In reviewing the results for values of strain on the order of 1 to 2 percent, it did not appear that this formed a rational basis. Typically, at higher confining stresses, the yield or inflection point observed in the stress-strain diagram occurs at higher strain, so it is not possible to pick a single strain value that appeared to be appropriate for each sample. The result would be that the failure envelope would have a very high cohesion intercept, and a low angle of internal friction.

As an alternate approach, an interpretation of failure for the triaxial specimens was based on observation of stress path diagrams (p-q diagrams) and selection of a point corresponding to the inflection where the curve begins to approach the  $K_f$  envelope. This approach is more subjective but results in lower shear strengths than would be selected if maximum shear stress or maximum principal stress ratios were used as failure criteria. The strain at failure, according to this definition, typically was around 5 percent.

Copies of stress path diagrams, stress strain diagrams, and summary data sheets for each of the relevant triaxial shear tests are included in Appendix C. A summary of the failure conditions for all is included in Table 4-2.

The results of the testing were used to interpret undrained strengths for total stress analysis and drained strengths for effective stress analysis.

#### **4.1.2.2.1 Undrained Strength of Silt and Clay**

It is assumed for the Milltown Bridge Infrastructure Mitigation project that the drawdown occurring after a flood, with the associated general scour and thalweg movement, will represent the worst-case assumption, and that undrained conditions will govern the stability of the slope.

Field vane testing was completed during the exploration. Field vane results are typically adjusted based on plasticity testing. Although much of the material at this site is non-plastic to low plasticity, there are occasional PI values ranging from 20 to 40. Therefore, a factor of 0.9 was used to adjust the shear strengths from vane shear testing. The results of the testing indicated undrained strengths ranging from about 525 psf to greater than 1,800 psf. The undrained strength is not an intrinsic property of the soil and varies with the stress conditions, the stress history, and other factors. Therefore, the results are more meaningful if considered as the ratio of the undrained strength to the effective vertical stress. The undrained strengths from vane testing correspond to undrained strength ratios of 0.9 and higher. These are very high, and probably represent a combined influence of silty and sandy interlayers, overconsolidated conditions, and borehole disturbance. It is not recommended



that these ratios be used to estimate the variation in shear strength (Table 4-3). They are reported here for comparison purposes only.

**TABLE 4-3**  
Vane Shear Testing Results

| Test ID      | Depth | Elevation (ft) | Undrained Strength (psf) | Undrained Strength Ratio |
|--------------|-------|----------------|--------------------------|--------------------------|
| SW1-3, VS-3  | 9.0   | 3241.0         | 600                      | 1.0                      |
| SW1-2, VS-5  | 15.6  | 3239.9         | 1,660                    | 2.3                      |
| SW1-3, VS-4  | 9.8   | 3240.2         | 525                      | 0.9                      |
| PB-2, VS-4   | 10.5  | 3248.5         | 695                      | 1.8                      |
| SW2-1B, VS-2 | 8.8   | 3245.1         | 590                      | 1.3                      |
| SW2-3, VS-1  | 6.5   | 3245.5         | 1,890                    | 5.1                      |
| SW1-2, VS-4  | 14    | 3241.5         | 975                      | 1.5                      |

The triaxial shear tests indicated undrained shear strengths ranging from 730 to 2,600 psf. Using only the samples that appear to correspond to normally consolidated conditions, the typical range of undrained strength ratio from the triaxial testing is 0.38 to 0.53, with an average value of 0.46.

The undrained strength to be used in stability analysis was estimated based on procedures recommended in the USACE Slope Stability Manual (USACE, 2003). These procedures were developed for use in dam analyses for rapid drawdown conditions. The USACE procedure is based on plotting the undrained strength on the failure plane in the triaxial specimen [calculated as  $(\sigma_{1f} - \sigma_{3f}) \cdot \cos(\phi') / 2$ , where  $\sigma_{1f} - \sigma_{3f}$  is the principal stress difference at failure] as a function of the consolidation stress, and using this to determine a shear strength envelope. This modified envelope has an intercept of  $d_{Kc=1}$ , and a friction angle of  $\psi_{Kc=1}$ . For each slice in the stability analysis, this envelope is used to relate the normal stress at the base to the shear strength. In the USACE procedure, the conditions before drawdown (i.e., the consolidation conditions) are evaluated to determine the effective normal stresses on the failure plane. Using these values, and the mobilized shear stress, the strength on the failure plane is interpolated between the undrained envelope described above, and the drained envelope.

In our analysis, for cases that the preliminary analysis indicated did not control the design, the analysis was completed using only the lower bound envelope from the USACE procedures, because this represents the lowest undrained strength. However, in the evaluation of sliding for the extreme limit state, it was necessary to interpolate between the two envelopes, as required by the USACE procedure, in order to demonstrate compliance with the design requirements.

Based on our evaluation following the USACE procedure, CH2M HILL used an undrained strength envelope with a cohesion intercept,  $d_{Kc=1}$ , of 213 psf, and a friction angle,  $\psi_{Kc=1}$ , of 18 degrees. This envelope represents the lower bound envelope in the USACE procedure.



#### **4.1.2.2 Drained Shear Strength of Silt and Clay**

The drained envelope for the sediment samples also varies depending on the failure criteria assumption. Using the procedure discussed above, CH2M HILL estimated an angle of internal friction ranging from 31 to 40 degrees for the sediment. A value of 31 degrees was generally used in the previous analyses.

#### **4.1.2.3 Residual Strength of Silt and Clay**

Because of a slope failure that occurred along the Contractor work pad on October 5, 2006, MDT has expressed concern over the residual strength of the sediment. The residual strength in this context is the strength occurring at very large strains, such as a previous failure surface. A discussion of the residual strength of sandy material was presented in a previous section of this report. The residual of clay is more complex and depends on the mineralogy, clay fraction, activity, and stress history, among other factors. Because of the wide range in possibilities, it is unlikely that the actual residual strength will be known without specific laboratory testing. However, some considerations include:

- The sediment material is typically non-plastic to low plasticity. Of the fine-grained samples tested (i.e., excluding the sand samples that comprise a significant part of the sediment unit) more than half are classified as non-plastic. For these materials, the difference between the effective stress friction angle and the residual stress friction angle is small (Stark and Eid, 1997).
- Clay and silt layers are present within the sediment unit that, on the basis of the index testing parameters, and the references previously discussed, could be subject to significant strength reductions along a previously established failure plane. Based on a liquid limit range of 40 to 60 percent, according to Stark and Eid (1997), the reduction in effective stress friction angle could range from 4 to 10 degrees. Theoretically, these reductions should be applied to the "fully-softened" strengths from the triaxial shear strength tests, which are much higher than the reduced strengths used in stability analysis to date.
- The reductions in shear strength may be incompatible with the reality of the observed conditions of stability subsequent to the initial failure. In other words, the steep slopes that remained after initial failure suggest that the reductions in shear strength were likely not significant, otherwise, continued progressive failure or deformation of the slope would have occurred.

#### **4.1.3 Alluvium**

The alluvium appears to consist of gravelly material, with some cobbles. Similar to the fill material, it is difficult to make estimates of the relative density or shear strength of this material because of the effect of the gravel and cobbles on the N-values. However, in our opinion, the N-values appear to indicate that the material is medium-dense to dense. Based on NAVFAC charts, a moist unit weight of 135 pcf, and an angle of internal friction of 38 degrees was estimated. Previous slope stability analyses by CH2M HILL used a total unit weight of 120 pcf, and an angle of internal friction of 35 degrees.



#### 4.1.4 Rock (Argillite)

Rock consisting of argillite was encountered below the sediment and alluvium layers. The rock is highly fractured or jointed. For the purposes of scour calculations, the rock was subdivided into an upper zone of poorer quality material overlying a slightly higher quality lower zone. However, in most of the slope stability calculations, the material has been considered as a high-strength material, and it is our opinion that slope failures through this material are unlikely. Therefore, our stability analysis included high values of cohesion to focus the search on potential failure surfaces through the soil layers.

For bearing capacity calculations, we treated the material as a single layer and developed equivalent cohesion and friction angles based on rock mass rating relationships.

The strength properties of the rock were based on a rock mass rating system as described earlier in this report (Bieniawski, 1998). CH2M HILL estimated the cohesion intercept and angle of internal friction for the upper more fractured rock (identified as "Type 1 Argillite" in our analyses). The parameters used in the stability analyses are shown in Table 4-4.

TABLE 4-4  
Fractured Rock Parameters

| Material         | Estimated Cohesion Intercept<br>(psf) | Estimated Friction Angle<br>(Deg) |
|------------------|---------------------------------------|-----------------------------------|
| Type 1 Argillite | 2100 to 4300                          | 15 to 25                          |
| Type 2 Argillite | 4300 to 6500                          | 25 to 35                          |

## 4.2 Slope Stability

The conditions include complex combinations of existing slopes, drawdown conditions, scour, undrained and drained conditions, etc. A summary of the cases for the slope stability analysis is included in Table 4-5.

Note that these stability analyses were performed prior to mobilization of a jet grouting contractor on the site. These analyses were generally completed with parameters that were discussed with MDT. The cross sections used in these analyses, and the findings are presented in Appendix D. As discussed in the previous section, some of these parameters will be revised as the design of stabilization measures is completed.

Jet grouting was not completed at the site, and the contractor demobilized from the site because of a slope failure that occurred on the work bench on the site. Because of concern over the stability of the working surface, interim riprap stabilization measures were undertaken. Additional analyses of the working conditions and the stabilization measures will be completed subsequent to this report.



## 4.2.1 Design Requirements

Our original calculations were performed to evaluate these conditions with respect to the AASHTO LRFD requirements (2006 Interim), assuming the jet grout mass is similar to a gravity retaining wall.

In the case of thalweg movement, the river could erode material from the toe of the slope at the face of the jet grout mass. In this condition, the function of the stabilization becomes similar to a gravity retaining wall. The jet grout mass is considered relatively impermeable; therefore, this condition becomes more critical during the recession of the flood level. If the thalweg movement occurs during a flood, then water may be trapped behind the mass, while the water in front of the mass recedes. Our analysis considered overturning, sliding, and bearing resistance for these conditions. The analyses are described in later detail for each of the respective cases.

**TABLE 4-5**  
Description of Stability Analysis Cases

| Case | Description   |
|------|---|
| 1    | Existing stability (I90 and SH 200), drained analysis   |
| 2    | Stability during drawdown and general scour (without stabilization, undrained and drained analyses) |
| 3    | Stability with general scour (and stabilization) – no rapid drawdown                                |
| 4    | Long-term stability   |
| 5    | Stability during drawdown after 100-year and 500-year floods, and thalweg movement                  |
| 6    | Seismic stability   |

After reviewing the originally submitted calculations, MDT requested that the evaluation be revised to present the results as a factor of safety. MDT requested that the jet grout stabilization meet minimum factors of safety of 1.3 and 1.1 when rapid drawdown is considered for the general scour and thalweg movement cases, respectively. MDT also requested that the stabilization provide a minimum factor of safety of 1.5 for long-term conditions.

## 4.2.2 Stability Analysis for Existing Conditions (Case 1)

The results of the stability analysis indicate that the existing conditions are relatively poor relative to the AASHTO LRFD standards (Table 4-6). It is likely that these results are slightly low because of the conservative strength parameters used. Particularly for the sediment layer, the existing slopes in the material suggest that a friction angle higher than 31 degrees could be used, or, an apparent cohesion may be providing some benefit. However, the conservative values have been used in the design to date, and these values provide a baseline for comparison.



**TABLE 4-6**  
Stability of Existing Conditions

| Location         | Factor of Safety |
|------------------|------------------|
| I90, West Side   | 1.02             |
| I90, East Side   | 1.24             |
| SH 200 West Side | 1.18             |
| SH 200 East Side | 1.08             |

### 4.2.3 Stability Analysis with No Stabilization Measures (Case 2)

The stability of the existing slopes was also evaluated for the scour and drawdown conditions so that the conclusions of the conceptual report could be reconsidered, and for comparison to the design of the stabilization measure (Table 4-7). These analyses reinforce the conclusions of the conceptual report that stabilization measures are necessary to protect the structure during drawdown and general scour.

**TABLE 4-7**  
Stability Analysis for Conditions with No Stabilization

| Location | Drawdown Stage | Scour Condition | Drainage Case | Factor of Safety |      |
|----------|----------------|-----------------|---------------|------------------|------|
|          |                |                 |               | West             | East |
| I90      | 1              | No Scour        | Undrained     | 0.91             | 1.18 |
|          | 1              | No Scour        | Drained       | 0.96             | 1.33 |
|          | 2              | General Scour   | Undrained     | 0.80             | 1.05 |
|          | 2              | General Scour   | Drained       | 0.76             | 1.10 |
|          | 3              | General Scour   | Undrained     | 0.80             | 1.11 |
|          | 3              | General Scour   | Drained       | 0.82             | 1.25 |
| SH 200   | 1              | No Scour        | Undrained     | 1.08             | 0.96 |
|          | 1              | No Scour        | Drained       | 1.27             | 1.12 |
|          | 2              | General Scour   | Undrained     | 1.00             | 0.91 |
|          | 2              | General Scour   | Drained       | 1.21             | 1.06 |
|          | 3              | General Scour   | Undrained     | 1.07             | 0.96 |
|          | 3              | General Scour   | Drained       | 1.30             | 1.13 |

### 4.2.4 Stability Analysis for Varying Water Levels (Case 3)

Cross Sections B and D, included in Appendix D were used for the west and east sides of I90, respectively, because they were the more critical section, determined based on the results of the analyses for Case 5 (Table 4-8). Also, these analyses only considered failure



through the jet grout mass. Other modes of failure, including sliding along a potential weak plane along the jet grout and rock interface were evaluated as part of the rapid drawdown analysis.

**TABLE 4-8**  
Stability Analysis for Case 3

| Location  | Ground Line   | Water Surface            | Lacustrine Sediment Strength | Factor of Safety |
|-----------|---------------|--------------------------|------------------------------|------------------|
| Section B | General Scour | Ordinary High Water      | Total Stress                 | 2.08             |
|           | General Scour | Ordinary High Water      | Effective Stress             | 2.41             |
|           | General Scour | 100-Year Flood Elevation | Effective Stress             | 2.35             |
|           | General Scour | 500-Year Flood Elevation | Effective Stress             | 2.64             |
| Section D | General Scour | Ordinary High Water      | Total Stress                 | 2.66             |
|           | General Scour | Ordinary High Water      | Effective Stress             | 2.97             |
|           | General Scour | 100-Year Flood Elevation | Effective Stress             | 3.15             |
|           | General Scour | 500-Year Flood Elevation | Effective Stress             | 3.19             |

#### 4.2.5 Stability Analysis for Long-Term Conditions (Case 4)

For long-term conditions, if a weak interface is assumed between the jet grout and the rock, the factors of safety are 1.6 and 1.9, respectively, for the west and east sides of the Blackfoot River, I90.

#### 4.2.6 Stability Analysis for Rapid Drawdown (Case 5)

Flood conditions appear to be the critical case for stability of the jet grout mass, because of the potential for undrained "rapid drawdown" loading as the water recedes from the flood levels. It is possible that the flood stage may build relatively slowly, compared to the rate at which the flood water recedes.

The "Case 5" Stability analyses considered the following conditions:

- General scour/rapid drawdown: This condition is assumed to include the loss of material caused by general scour along with rapid drawdown conditions. The total general scour depth was assumed to occur along the entire wetted perimeter, rather than tapering from the edges of the channel to the thalweg.
- Thalweg movement/rapid drawdown: This analysis represents the conditions that may exist if the river thalweg shifts to the face of the jet grout mass during a 100-year or 500-year flood, and is followed by relatively rapid drawdown.

For both of these conditions, we considered the potential for shear through the jet grout mass, and for sliding along an interface between the jet grout mass and the rock. For the thalweg movement case, we also considered overturning stability and bearing capacity. The



analyses were completed using limit equilibrium (Slide software), hand calculations (MathCAD), and finite element analyses (Plaxis).

#### **4.2.6.1 Rapid Drawdown Assumptions**

The sediment layer has been assumed to be mostly fine-grained in the stability analyses. Based on the consolidation test results, the coefficient of permeability is on the order of  $10^{-4}$  cm/sec. In order to saturate the sediment layer, water would need to flow through the jet grout mass, which will have a lower permeability, or through the sediment and alluvium along the sides and bottom of the embankment. Because of the long flow rates, and low permeability of the sediment and jet grout mass, it is anticipated that the rate at which the groundwater can rise within the sediment layer would be very slow. Based on simplified calculations using flow rates that could be expected under steady-state conditions, it is likely that the time required to fully saturate the area behind the jet grout mass could be on the order of hundreds of days. Therefore, the relative difference between the time leading up to the flood stage, and the time for the flood to recede appear to be relatively insignificant because little saturation of the embankment could occur during the flood stage. In our opinion, it is unlikely that the difference in water level between the river and the back side of the jet grout mass could be greater than several feet.

Our analysis considered a variety of water level elevations (behind the jet grout mass) to evaluate the limits under which the slope may maintain a factor of safety of 1.1.

#### **4.2.6.2 Shear Strength along Interface**

As a starting point in our analysis, it was assumed that there was no cohesion along the interface between the jet grout and the rock. However, it is anticipated that some cohesion strength will exist along the interface because the surface is unlikely to be planar, and because the jet grouting equipment will drill into the rock prior to beginning the jet grouting process. Because the surface of the rock is anticipated to include some poor-quality rock, our opinion is that the potential interface will be relatively rough, and that in order to fail by sliding, some shearing through the rock or jet grout material would have to occur. Therefore, we believe that it is appropriate to assume a cohesion component for the shear strength along the interface. After initially completing the calculations with no cohesion, we revised them to include cohesion of 1,200 psf, which is less than 10 percent of the strength of the jet grout mass.

#### **4.2.6.3 West Side of Blackfoot River, I90**

Under the combined general scour/rapid drawdown, and assuming that there is a weak interface, the estimated factor of safety for the west side of the Blackfoot River is 1.26, if a friction-only interface is assumed. The factor of safety when a cohesion intercept of 1,200 psf is considered is 1.36. If no weak plane is modeled, the factor of safety is estimated to be 1.80, with the worst-case groundwater assumptions.

For the thalweg movement case, using the worst-case rapid drawdown assumptions, analysis by Slide indicated a factor of safety of 1.06, even if the groundwater level is assumed to be at the highest level, and the interface is assumed to be only frictional strength. When the cohesion intercept of 1,200 psf is included, the factor of safety is estimated to be 1.29.



For the case where Slide was forced to generate only shear failures through the jet grout, the factor of safety was 1.63.

A separate analysis of the sliding and overturning modes was completed by using Slide to determine an earth force resultant on the jet grout mass. In this analysis, the portion of the cross section representing the jet grout was removed, and an earth force resultant was added. The magnitude of the resultant was varied, in order to find the value corresponding to a factor of safety of 1.0. This earth force resultant was then used in horizontal force and moment equilibrium calculations for the jet grout. These analyses indicated that in order to meet the desired factor of safety of 1.1 for the thalweg movement case, it is necessary that the water behind the jet grout mass be no higher than elevation 3254 feet, if the water at the face is assumed to be at elevation 3245 feet.

#### 4.2.6.3.1 Finite Element Analysis

In addition to the analyses above, a finite element analysis (Plaxis) was also performed for the cross section on the west side of I90. This analysis indicates that in order to maintain the factor of safety during the drawdown conditions, it is necessary to assume that the strength of the interface includes a cohesion component. A value of 1,200 psf was used in the Plaxis analysis. This is less than 10 percent of the expected strength of the jet grout mass (the portion in alluvium). This is still considered a conservative assumption, because it is not expected that a planar sliding surface will exist.

The finite element analysis indicated that a factor of safety of greater than 1.1 is maintained if the groundwater behind the jet grout mass is no higher than elevation 3252 feet, while the river level is at elevation 3245 feet.

**TABLE 4-9**  
Factors of Safety for General Scour, Rapid Drawdown Condition

| Cross Section  | Maximum Groundwater Elevation (ft) | Cohesion Intercept along Interface Layer (psf) | FS   |
|--|------------------------------------|--|------|
| I90 West, Cross Section B, General Scour (Slide Analysis)    | 3259                               | 1,200  | 1.36 |
| I90 West, Cross Section B, Thalweg Movement (Slide Analysis) | 3259                               | 1,200  | 1.29 |
| I90 West, Cross Section B, Thalweg Movement (Plaxis)         | 3252                               | 1,200  | 1.10 |
| I90 East, Cross Section D, General Scour (Slide Analysis)    | 3259                               | 0  | 1.41 |
| I90 East, Cross Section D, Thalweg Movement (Slide Analysis) | 3256                               | 1,200  | 1.10 |

#### 4.2.6.4 East Side of Blackfoot River, I90

In the general scour condition, the analysis of the east side of the river (I90) indicated a minimum factor of safety of 1.41 for the undrained, rapid drawdown case, if a frictional only



interface is included. Without the weak layer, the factor of safety is estimated to be 2.67 for the rapid drawdown, undrained case.

The analysis of the thalweg movement case for the east side of the Blackfoot River (I90) indicated a factor of safety less than 1.0 if the groundwater level is at elevation 3259 feet (while the river level is at elevation 3245 feet), and no cohesion is included. This calculation also includes higher unit weights for the fill material, as requested by MDT, and a higher friction angle chosen to correspond to the revised unit weight. Our opinion is that the assumptions for the groundwater level and interface strength are very conservative, and the calculations were only included as a starting point for understanding the conditions.

For the case with no cohesion, but lower groundwater levels, the factor of safety is 1.0 if the groundwater is at elevation 3252 feet while the river level is at elevation 3245 feet. If cohesion is considered (value of 1,200 psf) the estimated factor of safety is 1.10 if the groundwater level is no higher than elevation 3256 feet (while the river level is at elevation 3245 feet). Our opinion is that it is unlikely that the drainage conditions could create this condition, and that the design is therefore adequate.

For the case of shearing through the jet grout mass, analysis by Slide resulted in a factor of safety of 2.46.

Slide was also used to determine an earth force resultant for use in evaluating sliding and overturning resistance, as described for the analysis for the east side. The results of these calculations indicated factors of safety greater than 1.1, as long as the groundwater level is no higher than elevation 3254 feet, while the river is at elevation 3245 feet.

#### **4.2.7 Seismic Stability (Case 6)**

The stability analyses resulted in factors of safety of 1.15 and 1.42 for the west side and east side of the Blackfoot River, respectively. The analyses assumed that a weak interface exists (no cohesion intercept was included), and that general scour had occurred. The factors of safety represent acceptable conditions.

It should be noted that these stability analyses were completed based on the conclusion that most of the sediment material is fine-grained (silt and clay). It is now believed that much of the sediment layer is sandy. It is the opinion of CH2M HILL that liquefaction of sandy zones should be considered in the stability analysis during completion of design.

#### **4.2.8 Concluding Remarks on Stability Analysis**

The previous analyses indicated that the critical conditions affecting the stability of the jet grout mass are the amount of infiltration or drainage during a flood event, and the strength of the interface between the jet grout mass and the rock. Depending on the specific case evaluated, the analyses indicate acceptable conditions as long as the groundwater level is no higher than approximate elevation 3252 feet, when the river level recedes to elevation 3245 feet following the flood. It is also necessary to assume that the shear strength of the interface between the jet grout and the rock will include a cohesion component. The analysis indicates that the strength required is less than 10 percent of the anticipated strength of the jet grout within the alluvium. In the opinion of CH2M HILL, it is reasonable to assume some cohesion intercept because the rock is fractured, and the jet grouting equipment will drill



into the surface of the rock prior to beginning grouting. Therefore, in our opinion it is reasonable to assume that for sliding to occur at least a portion of the sliding plane would pass through the jet grouted material.

Subsequent to the completion of these stability analyses, a jet grouting contractor mobilized to the site and performed some jet grout test columns and production columns. This work was interrupted by a failure that occurred on the site on October 5, 2006, and the jet grouting contractor demobilized while interim stabilization measures were installed, as discussed previously in this report.

The slope stabilization design will be revised, based on observations of the jet grouting performed to date. Details of the design revisions will be presented in subsequent design reports.

It is anticipated that the following activities will be required to complete the revisions to the design of the stabilization measures:

- Evaluation of the suitability of jet grout, based on results from coring of test columns.
- Evaluation of the potential effects of the slope failure on the global stability of the slope, including the effects of softening of clayey material along the estimated failure plane.
- Evaluation of the stability of the site under construction loading, in order to develop more detailed requirements for the contractor performing the work.
- Stability analysis for seismic conditions, including the effects of liquefaction.



## 5.0 Embankment Settlement Evaluation

---

### 5.1 Settlement of Embankments

Each of the I90 and SH 200 Bridge structures include approach embankments that were constructed over loose and soft sediments. Therefore, it is likely that settlement of the embankments will occur during drawdown of the reservoir.

Estimates of settlement were made during the conceptual design, and were presented in the Mitigation Report (CH2M HILL, 2005). These previous estimates included a value of 2 to 3 inches of settlement at the northwest (west) abutment of the I90 structures, and approximately 1 to 2 inches of settlement at the southeast (east) abutment of I90. The estimated settlement at the SH 200 structures was 1 inch. These settlements considered only the compression of the sediments layer, because the fill material and the alluvium are generally coarse-grained and relatively incompressible.

Subsequent to the concept design, additional information on the subsurface profile and soil consolidation parameters was collected. Based on the final review of this information, it appears that the sediment layer includes generally more sandy material, which will be less compressible. The sandy layers will also consolidate much quicker than the clay layers. Since it appears that at least some of the sandy layers are present over significant lateral distances, their presence will also reduce the time of settlement for the finer-grained materials (silt and clay).

According to information from the EPA and Northwestern Energy, there have been significant extended drawdowns of the reservoir during previous decades. These drawdowns likely have had the effect of creating significant overconsolidation in the sediment material. This will reduce the magnitude of consolidation settlement.

Based on this information, a final settlement analysis has been performed to estimate the magnitude and duration of settlement for the project. This settlement evaluation included the following:

- Evaluation of the maximum thickness of silt and clay lenses or layers
- Evaluation of preconsolidation stress history for silt and clay layers
- Estimates of settlement magnitude
- Estimating the duration of settlement

Results from each of these evaluations are presented in the following paragraphs.

### 5.2 Thickness of Compressible Layers

The compressible silt and clay layers are the most compressible materials present within the sediment. Understanding the thickness of the compressible layers is important to the magnitude of settlement for any sublayer, and the duration of settlement.



Based on review of the soil boring logs provided by Envirocon, and the soil borings by CH2M HILL, it appears that the thickness of any individual clay layer is typically less than 6 feet. Generally, there are layers of sand, silty sand, or sandy silt present at the upper and lower boundaries of the materials.

If the sediment layer is to be evaluated as a single layer with "average" properties, in general it appears that no more than about one-half or three quarters of the sediment layer is composed of silt or clay material. The maximum thickness of the sediment layer beneath the embankments varies from about 10 to 25 feet at I90, to about 15 feet at SH 200.

### 5.2.1 Preconsolidation Stresses

The results of consolidation testing appear to indicate that the material is significantly overconsolidated. For example, the results for the samples recovered from soil boring EB-2, which is located southwest of the I90 bridges, indicate significant overconsolidation with depth. A summary of the estimated in situ vertical stress and the estimated preconsolidation stresses are presented in Table 5-1.

In general, this is consistent with the expectations because of the seasonal drawdowns and the significant drawdowns that have occurred in the past. As discussed in the following subsection regarding duration of settlement, the time required to reach a minimum of 90 percent of consolidation is estimated to be on the order of 40 days, based on the coefficient of consolidation estimates from lab testing, and the estimated thickness of layers. The 90 percent consolidation value is referenced because settlement is a logarithmic function, and the difference between 90 percent and 100 percent is theoretically large. However, even if the compressible layers do not even reach 90 percent consolidation it is almost certain that they would reach a minimum of 50 to 75 percent consolidation under the previous drawdowns. Therefore, our settlement estimates used an assumed typical preconsolidation stress based on a groundwater level at elevation 3250 feet. This is likely to represent a conservative estimate of the settlement.

**TABLE 5-1**  
Estimated Values of Maximum Past Vertical Stress ( $\sigma_p'$ )

| Sample      | Depth (ft) | Existing Effective Stress $\sigma_v'$ (psf) | Estimated Maximum Past Effective Stress $\sigma_p'$ (psf) |
|-------------|------------|---|---|
| EB-2, ST-1  | 2.1        | 79  | 1500  |
| EB-2, ST-2  | 4.0        | 150   | 1400  |
| EB-2, ST-8  | 19.7       | 740   | 2800  |
| EB-2, ST-9  | 21.3       | 800   | 5000  |
| SW1-1       | 20.2       | 357   | 1000  |
| SW2-1B, 3ST | 9.5        | 760   | 1500  |



### 5.2.2 Estimated Magnitude of Settlement

The magnitude of settlement varies depending on the assumed thickness of the different layers, and the preconsolidation stress. We prepared our estimate of settlement based on an assumption that about 75 percent of the sediment unit is composed of clayey material, and the other 25 percent is sandy material. The consolidation parameters were based on laboratory testing. For the sandy material, we used the low range of the laboratory testing results from the clayey material. The estimated settlement is presented in Table 5-2.

TABLE 5-2  
Estimated Settlement (primary consolidation)

| Location         | Estimated Settlement<br>(in) |
|------------------|------------------------------|
| I90 West Side    | 2-1/2 to 3                   |
| I90 East Side    | 1/2 to 1                     |
| SH 200 West Side | 1/2 to 1                     |
| SH 200 East Side | 1/2 to 1                     |

If it is assumed that most of the settlement is recompression, as a result of the significant reservoir drawdowns in the past, the settlement could be less than half the values presented above.

It should be noted that the above settlement estimates are based on the water level being lowered from the full pool elevation. However, at the time this report was prepared, the water level had been lowered to approximate elevation 3252 feet or lower for a period of at least 2 months. Therefore, some of the settlement should have already occurred.

### 5.2.3 Estimated Duration of Settlement

The calculation of the time of settlement can be made in relative simple terms, if based on the estimated height of drainage, and the coefficient of consolidation, as follows:

$$t = T \cdot H^2 / C_v$$

The parameter T is a dimensionless parameter that varies with the average degree of consolidation. Usually a value of 0.848 is used, corresponding to 90 percent consolidation. This is because consolidation theory is based on a logarithmic expression, and there can be a significant period of time between 90 percent and 100 percent consolidation.

Consolidation testing indicated relatively high values of the coefficient of consolidation,  $C_v$ , with most values above 1.5 ft<sup>2</sup>/day. As a conservative measure, our estimates of the time of consolidation were based on a value of 0.3 ft<sup>2</sup>/day.

The drainage height (H) is the thickness of the layer if single drained (i.e., a low permeability barrier at top or bottom of the layer), or half the layer height if the layer is double drained (soil at the top and bottom of the layer is relatively permeable).

The layer height was varied in calculations. Although we believe that there are so many sublayers of sand that the actual drainage height will typically be less than 5 feet, we performed a check calculation assuming a double-drained layer of 15 feet. This resulted in a time to 90 percent calculation ( $t_{90}$ ) value of 162 days. Therefore, in our opinion, the settlement caused by drawdown can be assumed to be essentially complete within about 6 months.

Another point that should be considered is that there have been significant drawdowns of the reservoir in the past. Even if these drawdowns only occurred over a period of a couple of months, it is likely that consolidation under these conditions reached at least 60 percent average consolidation. Therefore, it is likely that the settlement estimates presented above are very conservative.



## 6.0 Foundation Evaluation and Recommendations for Mitigation

---

Existing foundations were evaluated in the same groups that are being used for potential construction contract packages—that is, the I90 Abutments, the SH 200 Abutments, and the I90 and SH 200 central bridge piers (Pier 3 for each bridge). Each of the abutment foundations was evaluated and previously submitted in a technical memorandum separately for review. Any changes or modifications to the evaluation or recommendations are included in this section.

Other documents that pertain to this section include:

- Draft Technical Memorandum MRBM-01: Milltown Reservoir Bridge Mitigation, 2006 Geotechnical Exploration Summary. Dated May 26, 2006.
- Draft Technical Memorandum MRBM-02: Milltown Reservoir Bridge Mitigation, Pile Design Recommendations—I90 Abutments. Dated July 12, 2006.
- Draft Technical Memorandum MRBM-03: Milltown Reservoir Bridge Mitigation, Timber Pile Evaluation—SH 200 Bent Nos. 1, 2, and 5. Dated November 13, 2006.
- Technical Memorandum: Milltown Bridge Infrastructure Mitigation, SH 200 Piers 1 and 5—Timber Piles. Dated November 20, 2006.
- Technical Memorandum: Milltown Bridge Infrastructure Mitigation, I90 Pier 5—Steel Piles. Dated November 27, 2006.

### 6.1 I90 Abutment Evaluation

H-piles have been selected as the preferred method to be considered for underpinning the existing abutment foundations for the I90 westbound and eastbound bridges. The existing abutments require underpinning to counter the potential for either settlement of or excessive loading to the piles supporting the abutments during the lowering of the Milltown Reservoir. The new piles are being designed to provide axial capacity sufficient to support the abutment with minimal settlement and to resist drag loads from embankment settlement. For the I90 abutments, settlement resulting from drawdown of the reservoir is estimated to be 2 to 3 inches for the west abutments, and less than 1 inch for the east abutments (CH2M HILL, 2005). An updated and more complete discussion of abutment settlement is provided in Section 5.0 Embankment Settlement Evaluation.

Driven H-piles were selected as the preferred alternative to be considered for underpinning at the abutments, based on cost, constructibility (for example, ability to add length if refusal is deeper than expected), and the desire to minimize impacts to traffic on I90. H-piles will be driven to refusal through the approach embankments, reservoir sediments, alluvium, and terminate in argillite rock.

The abutment underpinning evaluation at I90 is presented in the following subsections that include:

- Subsurface profile, including estimated properties
- Pile design parameters, including: pile type, size and axial capacity, driveability evaluation, drag loads, LRFD factors, group effects, and estimated pile lengths

### 6.1.1 Subsurface Profile at the I90 Abutments

The subsurface profile at the abutments was developed based on the geotechnical explorations conducted at the site by CH2M HILL and others (CH2M HILL, 2005; CH2M HILL, 2006b). The generalized profile for design is summarized in Table 6-1.

**TABLE 6-1**  
Generalized Subsurface Profile

| Layer                | West Abutment                                |                    | East Abutment                                |                    |
|----------------------|--|--------------------|--|--------------------|
|                      | Elevation at Top of Layer<br>(ft, NAVD 1988) | Depth<br>(ft, bgs) | Elevation at Top of Layer<br>(ft, NAVD 1988) | Depth<br>(ft, bgs) |
| Embankment           | 3300   | 0                  | 3286   | 0                  |
| Lacustrine Sediments | 3260   | 40                 | 3260   | 26                 |
| Alluvium             | 3233   | 67                 | 3250   | 36                 |
| Argillite            | 3222   | 78                 | 3228   | 58                 |

Note: All elevations are based on the North American Vertical Datum, NAVD 1988.

Groundwater elevations at the abutments are assumed to be approximately equivalent to the adjacent reservoir pool elevation. At full pool, the reservoir pool elevation is 3261.8 feet. The predicted end-of-stage 1, stage 2, and stage 3 drawdown elevations are summarized in Table 3-5. A schedule showing the timing of the predicted drawdown and river level (Envirocon, 2005) is also attached to this report (see Appendix E). In addition, a plot of the existing and predicted vertical effective stress is given for each abutment and attached to this report (see Appendix E).

### 6.1.2 Subsurface Properties

The selection of subsurface properties for use in evaluating piles was completed during an earlier phase of the project. Soil parameters were selected for design based on evaluation of laboratory strength and index testing, and on observations and tests conducted during the field exploration. These parameters are summarized in Table 6-2.



**TABLE 6-2**  
Subsurface Properties

| Layer                                  | Unit Weight, $\gamma_m$<br>(pcf) | Cohesion Intercept, c<br>(psf) | Friction Angle, $\phi$<br>(Deg) |
|--|----------------------------------|--------------------------------|---------------------------------|
| Embankment                             | 120                              | 0                              | 35                              |
| Lacustrine Sediment (total stress)     | 90                               | 145                            | 18                              |
| Lacustrine Sediment (effective stress) | 90                               | 0                              | 31                              |
| Alluvium                               | 120                              | 0                              | 35                              |
| Argillite                              | 140                              | See Note                       |                                 |

Note: Shear strength properties for the argillite were evaluated based on rock mass characteristics, and presented in Section 3.2.8 Argillite Bedrock.

The parameters in Table 6-2 are generally consistent with those used in the stability analysis. However, as the evaluation of the stabilization measures continues, it is likely that the shear strength parameters used in stability analyses may be revised, as discussed in Section 4.0 Slope Stability Evaluation.

### 6.1.3 Pile Design Parameters

#### 6.1.3.1 Pile Type, Size, and Axial Capacity

H-piles were considered for underpinning, because of their higher resistance to damage driving through the alluvium layer, and their improved ability to penetrate into the argillite. H-pile section HP 14x117 was selected as the design section.

Piles driven into rock are difficult to assess axial capacity of the pile using theoretical methods because of uncertainties associated with depth of penetration, area of contact with the rock, and quality of the rock. It is likely that for piles driven to the argillite, either the need to protect the piles during driving, or the structural capacity of the pile will govern the design, instead of the bearing resistance of the rock. In other words, the piles will be driven to refusal in the rock, based on the limitations necessary to prevent overstressing of the steel.

It is recommended that all piles be fitted and driven with hardened steel drive shoes. Drive shoes need to be oversized, with a thickness that is approximately 0.5-inch greater than the thickness of the H-pile. This will help achieve good penetration into the argillite, and also reduce the soil to steel friction, thereby reducing drag loads.

The use of a pile driving analyzer (PDA) is recommended during driving because of hard driving at the toe and the need to monitor compressive stresses in the pile during driving. It is recommended that PDA testing be performed on a minimum of one pile at each abutment location.

#### 6.1.3.2 Drivability Evaluation

To evaluate the drivability of these piles, preliminary Wave Equation Analyses of Piles (WEAP) were performed to estimate the approximate size of hammer that will be required to install the piles without exceeding 90 percent of the yield stress of the pile. For



ASTM Grade A-50M steel, the yield stress is 50 ksi. For this analysis, it was assumed the pile would be driven to refusal. The preliminary analysis was based on a single-acting diesel hammer, with a corresponding manufacturer's rated energy range between 48 and 84 kip-feet.

Driving criteria should be developed in detail before the production piles are installed based on the contractor's actual driving equipment. It is recommended that the contractor be required to submit his actual hammer type and materials to the USACE. With this information, driving criteria can be developed by conducting a WEAP analysis of this equipment. Driving criteria will incorporate the contractor's planned equipment, and will be designed to achieve the required structural capacity of the pile.

#### **6.1.3.3 Drag Loads**

Drag loads were estimated based on an effective stress method ( $\beta$  method), assuming full mobilization of downdrag in the embankment and reservoir sediment layers. This is the most conservative approach for pile design, since the actual drag loads on the pile will likely be less than this value, depending on the soil-to-pile interaction in the embankment and reservoir sediment layers, following pile driving.

It is our opinion that the alluvium layer will not compress significantly following full drawdown. Assuming that the piles will be driven to refusal within the argillite layer, the evaluation assumes that drag will be generated within the embankment and sediment layers, and that the toe of the pile will remain fixed during consolidation of the reservoir sediments layer.

Drag loads were estimated for two cases:

- Case 1 assumes that a plug will form between the flanges of the pile during driving and partial soil to soil friction will occur during generation of drag loads.
- Case 2 assumes that no plug forms between the flanges of the pile, and that friction from drag loads are generated over the full surface area of the pile with soil to steel friction.

For each scenario evaluated (various water surfaces, geometries, etc.), the Case 2 analysis resulted in lower estimates of drag load. As such, the analyses indicate that the Case 2 condition is the weaker condition. In other words, it does not appear that the drag loads can reach the magnitude predicted by the Case 1 condition, because the soil would slip along the weaker soil to steel interface first and never fully mobilize the Case 1 friction.

Drag loads were estimated for full reservoir drawdown, or a Predicted End-of-Stage 3 Drawdown Water Surface (Envirocon, 2004a) of 3237.5 feet. This estimate was performed for both the existing piles at the I90 abutments (HP 10x42), and for the new piles (HP 14x117). The results are summarized in Table 6-3.



TABLE 6-3  
Drag Load Summary

| Pile Size | Estimated Unfactored Drag Load (kips) |               |
|-----------|---------------------------------------|---------------|
|           | West Abutment                         | East Abutment |
| HP 10x42  | 150                                   | 45            |
| HP 14x117 | 222                                   | 68            |

Note: Estimated loads are based on soil-steel interface friction values of  $0.5\phi$  (Kulhawy, 1984).

The estimated change in drag load from the Stage 1 water surface to the Stage 3 water surface is approximately 5 percent for the west abutment, and approximately 1 percent for the east abutment. Based on these drag loads, underpinning the east abutment to mitigate drag load due to drawdown may not be necessary, if structural evaluation shows the existing piles can handle existing dead and live loads, plus the estimated drag loads from Table 6-3.

#### 6.1.3.4 LRFD Resistance and Downdrag Load Factors

The recommended resistance factor is 0.58 ( $\phi = 0.65\lambda_v$ , where  $\lambda_v = 0.9$ ). Resistance and load factors were determined in accordance with LRFD Bridge Design Specifications (AASHTO, 2006). The resistance factor for the ultimate resistance of a single pile is based on capacity determined by wave equation analysis, with an assumed driving resistance and verified by simplified methods (for example, the PDA).

The load factor was selected based on the AASHTO LRFD Bridge Design Specifications, Interim 2006 version, but the code does not present options for effective stress-based design in granular soils. The AASHTO code allows for downdrag estimates for piles based on the  $\alpha$  Tomlinson Method or the  $\lambda$  Method. Based on reliability-based design according to the FHWA Design Guidelines for Resistance and Load Factor Selection for Driven Piles (FHWA, 1996), the recommended load factor is 1.4.

This load factor was selected based on the  $\alpha$  Tomlinson Method, which appears to be more conservative (and less reliable) than the  $\beta$  method, according to the FHWA guidelines. Therefore, while this load factor was not specifically developed for the  $\beta$  method used to evaluate drag loads on the piles, it is the most conservative option allowed by the AASHTO code.

#### 6.1.3.5 Lateral Resistance Input Parameters

The abutment foundations will experience lateral loads from earth pressures, traffic, wind, or seismic events. The pile and soil response to these loads can be modeled and evaluated using the program LPILE<sup>PLUS</sup>, Version 4.0 for Windows (Ensoft, 2000). To assist in this evaluation, the recommended LPILE input parameters are provided in Table 6-4. These parameters were taken from the LPILE User's Manual for the following soil layers:

1. Embankment material (model as "dense sand")
2. Reservoir Sediment (model as "soft clay")

The subsurface layers beneath the reservoir sediments do not need to be considered for the lateral analysis of the H-piles. Lateral behavior is not anticipated to be significant at these depths. Groundwater was modeled at the top of the sediment (near normal operating pool).

**TABLE 6-4**  
Recommended LPILE Input Parameters

| Layer               | $\gamma_r$<br>(pcf) | k<br>(pci) | $\phi$<br>(deg) | $S_u$<br>(psi) | $\epsilon_{50}$<br>(dim) |
|---------------------|---------------------|------------|-----------------|----------------|--------------------------|
| Embankment          | 120                 | 20         | 35              | 0              | 0.005                    |
| Lacustrine Sediment | 90                  | --         | --              | 7              | 0.01                     |

### 6.1.3.6 Group Effects Evaluation

Group effects for vertical and lateral loads were considered between the new piles and the existing piles. The existing piles are spaced at 8-foot, 4-inch center-center spacing. The new piles are spaced at 6-foot center-center spacing, with the exception of the center pair spacing of 5 feet. The nearest diagonal distance between new piles and existing piles is approximately 3.5 feet, although in most locations it is 5 feet or greater.

Because of this layout, and in combination with how forces will be developed at the abutment, group effects for drag loads are not anticipated to control over drag loads of individual piles. For lateral loads, the group effects should be considered if the spacing in the line of loading is less than five equivalent diameters, following recommendations in the AASHTO LRFD Bridge Design Specifications.

### 6.1.3.7 Estimated Pile Lengths

Pile lengths were estimated based on the generalized subsurface profile in Table 6-1, and a minimum penetration of 3 feet into the argillite. The assumed penetration to reach refusal in argillite is 15 feet. Estimated pile lengths are summarized in Table 6-5.

**TABLE 6-5**  
Estimated Pile Lengths

| Parameter               | West Abutment                   | East Abutment |
|-------------------------|---------------------------------|---------------|
| Pile Type/Size          | Steel H-pile, Section HP 14x117 |               |
| Minimum Toe Elevation   | 3219                            | 3225          |
| Estimated Toe Elevation | 3207                            | 3213          |
| Estimated Pile Length   | 89 feet                         | 69 feet       |

Note: Pile head is assumed to be approximately 4 feet below the ground surface, based on current drawings and 2 feet of embedment of the pile head into the cap.

### 6.1.4 Concluding Remarks on I90 Abutments

Using the drag loads summarized in this section, structural evaluation of the existing piles suggests that underpinning of the west abutment is necessary, in order to mitigate for



reservoir drawdown. This conclusion is also supported by the magnitude of abutment settlement that has been measured by MDT at the west abutment. Structural evaluation of the existing piles at the east abutment suggests that they have sufficient structural capacity to handle the drag loads, using drag loads in Table 6-3.

The drag loads summarized in Table 6-3 are for the effective stress method described in this section. Evaluation with other methods was also performed, including the Nordlund method (FHWA, 1996) and a total stress analysis. Although the magnitude of drag load varied widely for the methods used, the change in drag load (from existing conditions to post-drawdown conditions) was consistently small. The change in drag load estimated at the east abutment is less than the change in drag load estimated at the west abutment (see Technical Memorandum summarizing structural recommendations at the I90 abutments, dated November 27, 2006), primarily because of the thinner layer of reservoir sediments at this location.

It is understood that MDT may not agree with the conclusion that the piles have already experienced drag loads. Records of the past magnitude of reservoir drawdown, and measurements of settlement at the east abutment, suggest that the piles have performed sufficiently and have likely been subjected to drag loads that approach the magnitude that will result following full drawdown of the reservoir.

## 6.2 SH 200 Abutment Evaluation

Pile resistance and drag loads were estimated for the existing piles at the SH 200 bridge, for Bent Nos. 1, 2, and 5. These bents are founded on dual timber-pile-supported pile caps, constructed in 1950. Bent Nos. 3 and 4 are founded on spread footings. The layout of each footing and the pile spacing are shown in the as-built drawings, included in Appendix E.

The piles at SH 200 are treated timber piles, with a diameter of 12 inches. Although it is not clear on the as-built drawings, it is assumed that the 12-inch-diameter is for the pile butt. The pile lengths at Bent Nos. 1 and 5 are 40 feet; at Bent No. 2, the pile length is 30 feet (see Appendix E). The as-built drawings included in the Mitigation Report (CH2M HILL, 2005) indicate that all piling "*shall be driven to carry a load of 21 tons [42 kips] per pile*"; which is the allowable design load, or unfactored load, for these piles. In order to evaluate whether these piles are structurally capable of carrying additional load brought on by reservoir drawdown, the ultimate resistance and drag loads were estimated for final (Stage 3) reservoir drawdown.

Ultimate resistance and drag loads were estimated by the effective stress ( $\beta$ ) method. Based on the timber pile specification in effect at the time of construction (ASTM D25), and the Timber Pile Design & Construction Manual (Timber Piling Council, 2002), the piles were modeled with a 0.8 percent taper (0.1 in/ft). This value was selected because it is conservative, in that it results in a higher drag load than a greater pile taper.

For these analyses, the taper was considered only during the determination of circumferential area used in the drag load computation. No allowance was made to include relaxation that might occur as soil "settles away from the pile." By "settling away," the soil is assumed to settle downward in a vertical plane, but the pile surfaces taper away from this plane. In principal, this should result in some relaxation that results in reduction in the